Sustainable Cities and Society 143 (2026) 107364

Contents lists available at ScienceDirect

Sustainable Cities and Society

journal homepage: www.elsevier.com/locate/scs

When to stop? A visual impact assessment framework for incremental urban and community expansion in rural heritage landscapes

Yuyang Peng [a], Steffen Nijhuis [b], Zhuoyue Wang [c], Yingwen Yu [c,*], Edward Verbree [c], Peter van Oosterom [d]

[a] Department of Urbanism, Delft University of Technology, Julianalaan 134, Delft, The Netherlands
[b] Head of the Section Landscape Architecture, Full Professor of Landscape-based Urbanism, Department of Urbanism, Delft University of Technology, Julianalaan 134, Delft, The Netherlands
[c] Department of Architectural Technology and Engineering, Delft University of Technology, Julianalaan 134, Delft, The Netherlands
[d] Head of Section Digital Technologies, Full Professor of GIS Technology, Department of Architectural Technology and Engineering, Delft University of Technology, Julianalaan 134, Delft, The Netherlands

ARTICLE INFO

Keywords:
Urbanization
Visual impact
Cultural landscape
Point cloud
Street view imagery (SVI)
VR eye-/head-tracking
3D Gaussian Splatting (3DGS)

ABSTRACT

Incremental urban and community expansion in rural heritage landscapes often produces cumulative visual impacts, yet planning rarely specifies a clear endpoint for acceptable change. This paper proposes an integrated Visual Impact Assessment (VIA) framework, aligned with SDG 11, to determine "when to stop" using stage-comparable evidence across past, present, and future conditions. The framework is organized in three modules. First, a point cloud-enhanced GIS module quantifies visibility and spatial change across development stages. Second, an enhanced Key Observation Point (KOP) module derives matched eye-level evidence from multi-temporal street-level panoramas and scenario visualizations, for example using Street View Imagery (SVI) time series and 3D Gaussian Splatting (3DGS) rendering. Third, a decision layer integrates structured public acceptability from a questionnaire covering different respondent groups with in-depth expert interviews and synthesis, with virtual reality (VR) eye- and head-tracking used as supportive behavioral evidence. Applied to the Middenbeemster expansion in the Beemster Polder, the Netherlands, the framework yields a case-calibrated reference package for decision support: KOP-based construction intensity serves as the primary reference line for review, perception indicators serve as supporting guardrails, spatial character metrics act as case-specific reference checks to protect the polder framework, and visibility diagnostics remain a necessary screening layer. More broadly, the framework provides a transparent and replicable procedure that can be transferred and locally recalibrated for heritage-sensitive rural-urban fringes where change is incremental and cumulative, supporting a stage-comparable VIA approach.

1. Introduction

In recent decades, global urbanization and the outward expansion of settlements have accelerated; by 2050, nearly 70 % of the world's population will live in urban areas (Desa, 2006). Urban expansion in peri-urban and suburban areas has emerged as a dominant spatial process (Xue et al., 2025), reshaping the visual environment and the sense of place in suburban and rural landscapes (La Rosa et al., 2018; Tan et al., 2024). Many of these landscapes embody cultural and heritage values and can be understood as rural heritage landscapes, that is, "combined works of nature and humankind" shaped through long-term human–environment interaction and perceived through everyday experience (Bridgewater & Rotherham, 2019; Scazzosi, 2018). They archive agrarian spatial patterns and historic hydraulic networks and deliver cultural ecosystem services such as place attachment, aesthetic experience, and recreation (Aimar, 2024; Assessment, 2005; Zhang & Stewart, 2017). International guidance and professional practice, including SDG 11 (SDG 11; Sustainable Cities and Communities) (Falah et al., 2025), also emphasize safeguarding cultural and natural heritage and call for systematic impact assessment during planning and design (Bond & Worthing, 2016; Pereira Roders & van Oers, 2012). In practice, however, low-intensity, incremental urban expansion, such as the

* Corresponding author.
E-mail addresses: Y.Peng-1@tudelft.nl (Y. Peng), S.Nijhuis@tudelft.nl (S. Nijhuis), Z.Wang-111@student.tudelft.nl (Z. Wang), Chirstinayu@tudelft.nl (Y. Yu), e.verbree@tudelft.nl (E. Verbree), p.j.m.vanoosterom@tudelft.nl (P. van Oosterom).

https://doi.org/10.1016/j.scs.2026.107364
Received 29 September 2025; Received in revised form 31 March 2026; Accepted 1 April 2026
Available online 2 April 2026

gradual spread of small clusters of low-rise, community-oriented housing at the urban fringe, is the most common form of edge growth yet is often overlooked (Echenique et al., 2012; Soltani et al., 2025). These changes are less conspicuous than landmark buildings or wind turbines and therefore tend to escape early scrutiny (Ravetz et al., 2013). Their cumulative effects produce visible degradation that is difficult to define and manage (Gazzola et al., 2018). This makes evidence-based "when to stop" limits a practical planning need for peri-urban rural heritage landscapes (Bailoni et al., 2012).

Visual Impact Assessment (VIA) is the internationally adopted tool for addressing this problem (Fisher, 1993; Oxman, 1997; Wu et al., 2026). It typically combines GIS-based viewshed analysis (Wróżyński et al., 2024), photomontage (Zube et al., 1987), and 3D simulation to model change (Ervin, 2001), then compares existing, proposed, and future scenarios from key observation points (KOPs) and along moving viewpoints (Jin, 2023; Peng & Nijhuis, 2021). Public perception and expert judgment are integrated into an overall appraisal (Han et al., 2025). Although the workflow is relatively mature, VIA practice and scholarship have largely concentrated on visually salient object types, including transport infrastructure (Jaeger et al., 2011; Sangiorgi & Irali, 2012), energy facilities (Apostol et al., 2016; Dower, 2020; Florio et al., 2021), and high-rise or modern insertions (Yuan et al., 2024; M. Zhao et al., 2020).

Despite growing experience, several gaps remain central to the study and practice of VIA for low-intensity incremental expansion, where common low-rise accretive change is subtle, cumulative, and often difficult to detect with standard DEM (Digital Elevation Model)-based viewsheds or snapshot KOP approaches (Penko Seidl & Golobič, 2020; Zeng et al., 2023). Existing frameworks also rarely anticipate how accretive change shifts perception over time, and they seldom provide transparent decision-support reference points, such as stop rules or threshold bands that can inform mitigation, redesign, or a pause once cumulative change approaches or exceeds an acceptable envelope (Johnson & Ray, 2021; Llausàs et al., 2016; Proverbs et al., 2020). In addition, despite advances in immersive methods, point clouds, and real-time rendering, many applications still rely on DEM-based GIS or static KOP imagery, limiting evaluative granularity and integration across evidence streams (Habib et al., 2024; Lu et al., 2023; Y. Peng et al., 2026; Peng et al., 2022).

Therefore, this paper proposes and applies an integrated VIA framework to address these gaps. The framework is designed to: (i) link historical change, current conditions, and future scenarios to evaluate cumulative impacts of incremental expansion and identify a case-calibrated reference range for visual acceptability; (ii) integrate point cloud-supported GIS analysis with eye-level perception evidence, so that area-scale exposure and experiential effects can be assessed in a comparable structure; and (iii) connect public evaluation with expert synthesis to translate acceptability signals into a structured stop-rule procedure and locally calibrated reference bands for decision support. The framework is tested through staged community expansion scenarios in the Beemster Polder, the Netherlands. This paper makes two contributions: methodologically, it extends VIA to better capture cumulative and temporal change across incremental stages through a procedure that can be transferred and locally recalibrated; practically, it provides a structured basis for planning and heritage-management decisions, with locally grounded stakeholder participation remaining an important direction for future application.

2. Towards an integrated VIA framework for urban expansion

Environmental assessment (EA) systems vary internationally, but many jurisdictions distinguish plan-level assessment, often termed strategic environmental assessment (SEA), from project-level assessment, often termed environmental impact assessment (EIA), with screening procedures determining whether an assessment is required. Within these workflows, VIA is commonly treated as one component of EA, either reported as a dedicated chapter within EIA or SEA documentation or requested during permitting as supporting evidence. Importantly, in contexts where cultural and heritage attributes are prominent, impacts on landscape's visual-spatial character and heritage setting can warrant dedicated scrutiny. In such cases, VIA, or a setting-focused review, may be required as a stand-alone assessment even when a full EA procedure is not triggered, reflecting the higher sensitivity of the receptor and the need for transparent mitigation and design iteration. Accordingly, this section first reviews established VIA frameworks, then identifies opportunities for methodological enhancement, and finally presents the integrated framework proposed in this study.

2.1. Conceptual foundations

Wide-applied VIA frameworks (Table 1) comprise two methodological clusters and one decision layer. The two clusters correspond to complementary ways of analyzing visibility and perception, while the decision layer links evidence to planning and management decisions (Cilliers et al., 2023):

(a) Viewpoint-based assessment: Typically conducted through KOP analysis, using photomontages, 3D visualizations, or rendered interventions, followed by expert appraisal or public preference testing (Lange, 2011; Paar, 2006). Its strength lies in communicability, but it is often snapshot-based and relies heavily on subjective judgment, which limits sensitivity to subtle incremental change (Bishop & Rohrmann, 2003).

(b) GIS-based visibility and spatial analysis: Based on terrain and land-cover representations, ZTV (Zone of theoretical visibility) and viewshed computations map potential exposure at area scale, and index models can integrate coefficients such as visible-object counts, affected-settlement shares, observer distance and orientation, and exposed population (Cimburova & Blumentrath, 2022; Domingo-Santos et al., 2011; Peng et al., 2025). These methods are powerful for cumulative exposure and large footprints, yet inconspicuous, gradually expanding change remains difficult to capture (Palmer, 2022; Wróżyński et al., 2016).

Table 1
The summary of the widely applied VIA or VIA-related frameworks.

Framework / Guidance	Primary focus	Core method features
BLM Visual Resource Management (contrast rating)	Viewpoint (KOP)	Elemental contrast judgment (form, line, color, texture) at representative viewpoints; standardized field sheets
Berkeley contrast rating (Palmer, 2022)	Viewpoint (KOP)	Numeric scaling of elemental contrasts; composite indices across views/options
GLVIA (LVIA)	Viewpoint (KOP) + GIS	Photomontage/visualization at KOPs; sensitivity (susceptibility + value) × magnitude → significance; ZTV screening
SP2 (wind-farm visibility index) (Palmer, 2022)	GIS	Multi-coefficient spatial model (visibility count, affected buildings, distance, orientation, population)
SAM (AUS)	Public metrics at viewpoints (KOP)	Large-sample preference model; significance tests for preference drops at representative views
Maine Wind Energy Act (WEA) guidelines	Mixed (GIS + KOP + public)	Statutory multi-criterion test (resource value, project scale, extent/duration, user expectations, continued enjoyment)
HIA for World Heritage	Value–expert judgement	Identifies effects on OUV attributes and setting; uses KOPs/ corridors; may include GIS

(c) Decision layer: This interprets and integrates evidence into policy-legible conclusions through public evaluation and value-based or expert judgment (Daniel, 1976). Public evaluation anchors judgments in social acceptability via structured instruments at representative viewpoints, while expert judgment interprets evidence in relation to landscape sensitivity, statutory objectives, and landscape or heritage attributes (Berry et al., 2010).

2.2. Technical underpinnings

VIA depends on data and tools, and several limitations of conventional workflows can be mitigated by integrating newer techniques across evidence streams. In this study, we introduce four complementary technologies to overcome these limitations:

(a) Point cloud-based GIS visibility and spatial analysis: Airborne LiDAR and terrestrial or mobile laser scanning generate point clouds that represent terrain, vegetation volumes, and built mass as explicit 3D geometry (Bai et al., 2021; Y. M. Zhao et al., 2020). This better captures occlusion by canopies and facades and reduces bias from bare DEM or DTM (Digital Terrain Model) viewsheds, improving visibility and spatial analysis precision (Bai et al., 2021; Marešová et al., 2024).
(b) Street View Imagery (SVI) with semantic segmentation: Multi-temporal, geo-referenced panoramas enable eye-level monitoring of incremental change; semantic segmentation produces indicators such as building or paving share, Green View Index, and sky ratio (Biljecki & Ito, 2021; Middel et al., 2018). These can be combined into construction-intensity indicators and compared across periods, and panoramas can also serve as stimuli in perception experiments (Peng et al., 2026b; Stalder et al., 2024; Xu et al., 2024).
(c) 3D Gaussian Splatting (3DGS) for scene rendering: Traditional photomontage fixes the views, and large mesh renders are heavy and artefact-prone (Kerbl et al., 2023). 3DGS supports real-time free-view rendering from dense imagery and point clouds, preserving material cues while enabling interactive exploration, and can be used to create comparable present and future visualizations (Wang et al., 2025; Wen et al., 2025; Yu et al., 2025a,b; Yuan et al., 2024; Zeng et al., 2023; Zhang & Stewart, 2017; M. Zhao et al., 2020a; Y. Zhao et al., 2020b; Zong et al., 2021; Zube et al., 1987).
(d) Immersive VR with eye- and head-tracking: Visual impact ultimately concerns human perception (Moreno-Arjonilla et al., 2024). Immersive VR enables embodied exploration and records gaze and head-motion measures that quantify attentional salience and cognitive effort, strengthening human-level evidence beyond 2D preference ratings (Stalder et al., 2024; Stein et al., 2024).

In summary, point cloud analysis improves spatial precision; SVI time series capture incremental and cumulative change; 3DGS enables high-fidelity free-view rendering; and VR with eye- and head-tracking strengthens human-level evidence.

2.3. Proposed VIA framework

Following the prevailing VIA framework, the proposed framework is organized into three components that correspond directly to the two evidence streams (a-b) and the decision layer (c), while also embedding a temporal perspective (Fig. 1). It aligns evidence across past (accumulated incremental change), present (current impact levels), and future (development options), enabling cross-temporal comparison and cumulative impact identification.

(a) GIS analysis enhanced by point clouds (evidence): Its objective is to identify where the project is visible, how strongly, and for whom, while also detecting how new interventions affect spatial composition and structural indicators (Bai et al., 2021). The analysis, therefore, addresses three layers: the direct impact of new elements on the landscape, their cumulative overlay with existing elements, and their influence on human activity spaces such as roads, open fields, or settlement edges (Peng et al., 2024). Historical incremental change is detected and quantified by comparing successive airborne LiDAR point clouds (e.g., AHN-3/4/5). Differences in built and vegetation height surfaces and class masks are summarized as incremental exposure change and incremental spatial-structure change. These high-resolution datasets allow temporal change to be measured directly and consistently across periods.

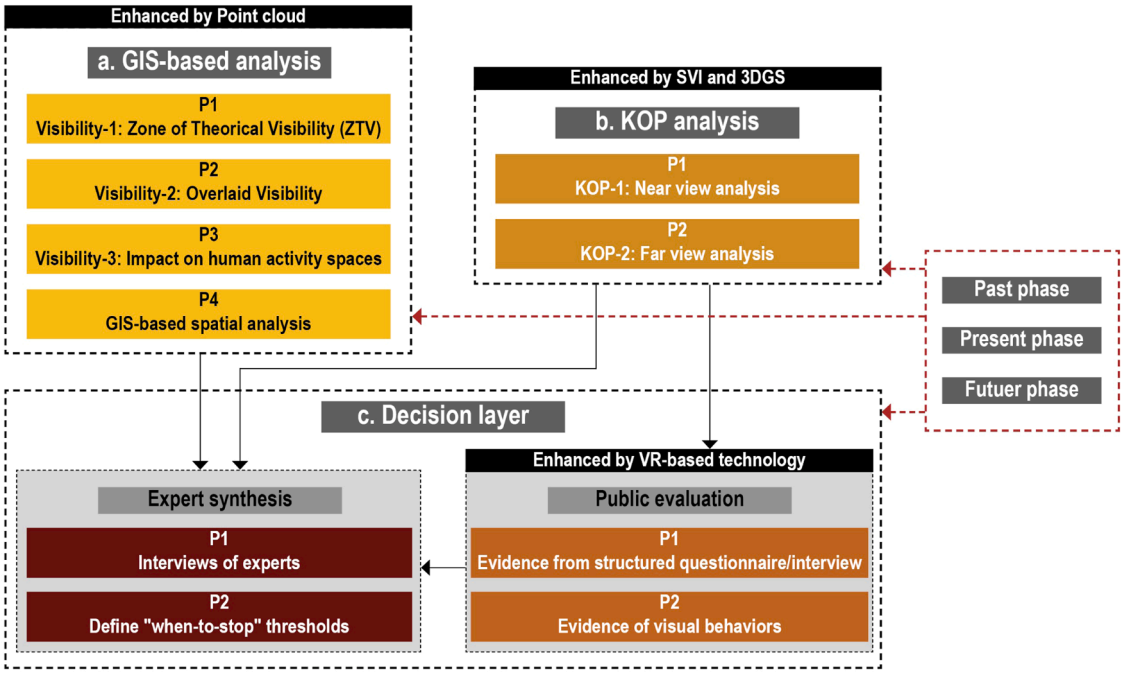

Fig. 1. The main compositions of the newly proposed VIA framework.

(b) Enhanced KOP analysis (evidence): Multi-date SVI provides time-series indicators of construction intensity and its change, while 3DGS supports consistent, eye-level visualizations of present conditions and future patterns under controlled viewpoint settings (Xia et al., 2021). Together, these sources enable stage-comparable KOP evidence across past, present, and proposed scenarios by extracting the same indicator family from matched viewpoints. This allows incremental and cumulative eye-level change to be quantified from different time series.

(c) Public evaluation and expert synthesis (decision layer): Public perception is elicited through structured preference scales and short interviews, and immersive VR experiments can provide supporting physiological evidence (eye and head metrics) to corroborate salience and exploration patterns (Moreno Arjonilla et al., 2024). Expert assessment then integrates these inputs with statutory frameworks and site attributes. The synthesis compares evidence across time slices to identify where change approaches a low-acceptability range, and derives limiting indicators as stop-rule reference bands and decision-support criteria (Gravagnuolo et al., 2024). By reading public responses and supporting VR evidence against the same time slices, the decision layer can locate where acceptability drops and translate that point into practical review bands and mitigation cues.

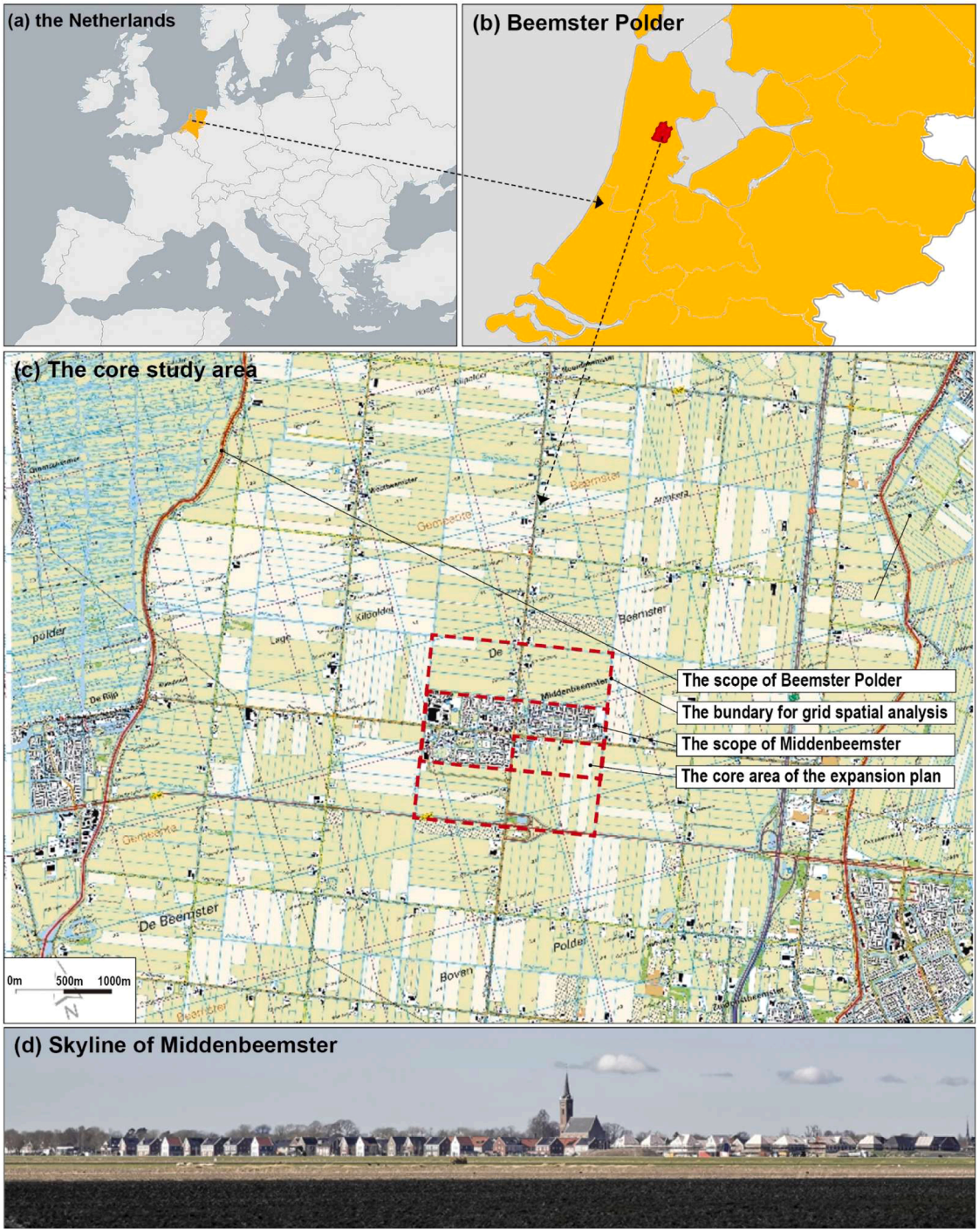

Fig. 2. Middenbeemster expansion plan and Beemster Polder: the location of the targeted study area.

3. Case study: Expansion of Middenbeemster in Beemster polder

3.1. Background of the case study

Framed as a long-range response to housing pressure and service deficits in the Beemster municipality, the Middenbeemster Expansion Plan (2020–2040) sets out a phased program of urban growth in and around De Keyser II (Fig. 2). It combines new housing and community facilities with selective redevelopment and the reuse of green parcels. Conceived to accommodate rising residential demand, the plan's interventions are intentionally incremental, gradually transforming existing farmland into low-rise but more concentrated residential communities. At the same time, the plan unfolds within the Beemster Polder, a canonical Dutch polder landscape created in 1612 through the drainage of lakes and organized into a strict geometric grid of canals, dikes, roads, and agricultural plots. This rational agrarian order is highly sensitive to spatial and visual disturbance. The area is also inscribed on the UNESCO World Heritage List, underscoring its international recognition (Renes, 2019).

These circumstances highlight a central tension between conserving a rural heritage landscape and accommodating local community growth. The key question is how to assess the visual effects of the ongoing expansion on the surrounding polder landscape, particularly because such effects are not sudden but accumulate gradually over time. In this context, potential impacts may include the progressive interruption of long-distance sightlines, a shift in perceived openness and horizontality, and increasing visual dominance of built mass at both settlement edges and everyday eye-level viewpoints. Against this background, the Middenbeemster case provides an appropriate testbed for applying the integrated VIA framework and examining past cumulative change, present conditions, and prospective scenarios across the plan's phased implementation.

3.2. Data collection

This study relies on three primary categories of data (Table 2): (a) point cloud data for visibility analysis, (b) multi-view imagery and scan data for 3DGS rendering, and (c) SVI and panoramic photos for temporal analysis. These datasets enable a cross-temporal assessment of past, present, and prospective impacts. The AHN and Google SVI datasets are publicly available, ensuring transparency and reproducibility. Drone imagery and X-Grid L1 multi-angle imagery and sparse point clouds were collected to support high-fidelity 3DGS scene reconstruction for VR perception experiments. In addition, multi-angle imagery and point cloud data were acquired for three proposed construction scenarios; the imagery was used to create 3DGS virtual environments, while the point clouds supported visibility analysis across alternatives.

Table 2
Summary of the research data.

Data	Data type	Source/ acquisition	Description and use
AHN 3–5 (Actueel Hoogtebestand Nederland)	Point cloud data	Open-access	Dutch national airborne LiDAR program (AHN) has produced repeated, country-wide point clouds at multi-year intervals since 1996 (AHN1–AHN5). In this study, AHN-5 (2023; raw and classified/edited variants) is used as the baseline for visibility and spatial-metrics analyses, while AHN-3 (2015) and AHN-4 (2020) are used for comparable spatial analyses to represent earlier conditions and support temporal comparison.
Drone aerial images	Image data	DJI Mini 2	Collected to generate 3D Gaussian Splatting (3DGS) renderings, construct scenario scenes, and provide inputs for VR perception experiments.
Multi-angle images and sparse point clouds	Image and point cloud data	X-Grid L1	Acquired to create high-fidelity 3DGS visualizations, support hypothetical scenario construction, and complement VR experiments.
Google SVIs	Image data with geolocation	Open-access	High-resolution panoramas are used for temporal analysis of cumulative changes. Multi-date images were selected from comparable seasons to minimize confounding due to vegetation cycles.

4. Methods

Building on the proposed VIA framework, we assess cumulative and prospective visual change in/around Middenbeemster by combining three temporal stages (past, present, and future). The analysis follows the framework's three components: point cloud-supported GIS visibility and spatial metrics, enhanced KOP analysis, and decision layer, public evaluation with expert synthesis (Fig. 3).

4.1. GIS visibility and spatial metrics (point cloud-enhanced)

The first analytical component applies a point cloud-enhanced GIS workflow to quantify the visual impacts from the past to proposed constructions. The workflow comprises three visibility steps (GIS-1 to GIS-3) plus one spatial-character step (GIS-4):

(a) Model construction: The workflow commenced with creating a baseline model based on the AHN-5 (the most recent release covering the study area) national LiDAR point cloud dataset. This AHN-5-based baseline represents terrain morphology, vegetation volumes, and existing built mass in explicit 3D geometry, thus avoiding the "bare-earth" bias of DEM/DSM-based viewsheds. On this baseline, three proposed development scenarios (M-1–M-3) were generated by positioning building segments extracted from representative local structures (Fig. 4). In addition, earlier national LiDAR releases (AHN-3, 2015; AHN-4, 2020) were used to quantify recent spatial changes in terrain/vegetation/built features and to inform the change analysis.

(b) Visibility computation (GIS-1/2/3): Visibility calculations were carried out in ArcGIS Pro using cumulative raster-based viewshed analysis. Integrated terrain-building surfaces were rasterized to 1-m cells, balancing computational efficiency with the resolution required for fine-scale heritage landscape analysis.

For Activity-oriented visibility (GIS-3), observer points were placed every 5 m along road centerlines around De Keyser II. Road receptors were referenced to the LiDAR-derived bare-earth DTM with a 1.7 m vertical offset (DTM + 1.7 m) to represent ground-based viewpoints. The occluding surface was constructed by rasterizing the maximum height per 1 m cell from building and major-vegetation classes, with low vegetation filtered to avoid shrub-level noise. Line-of-sight obstruction was evaluated on this integrated surface, thereby capturing screening without placing viewpoints on canopy-level surfaces.

For cumulative visibility (GIS-1/2), building-surface sample points

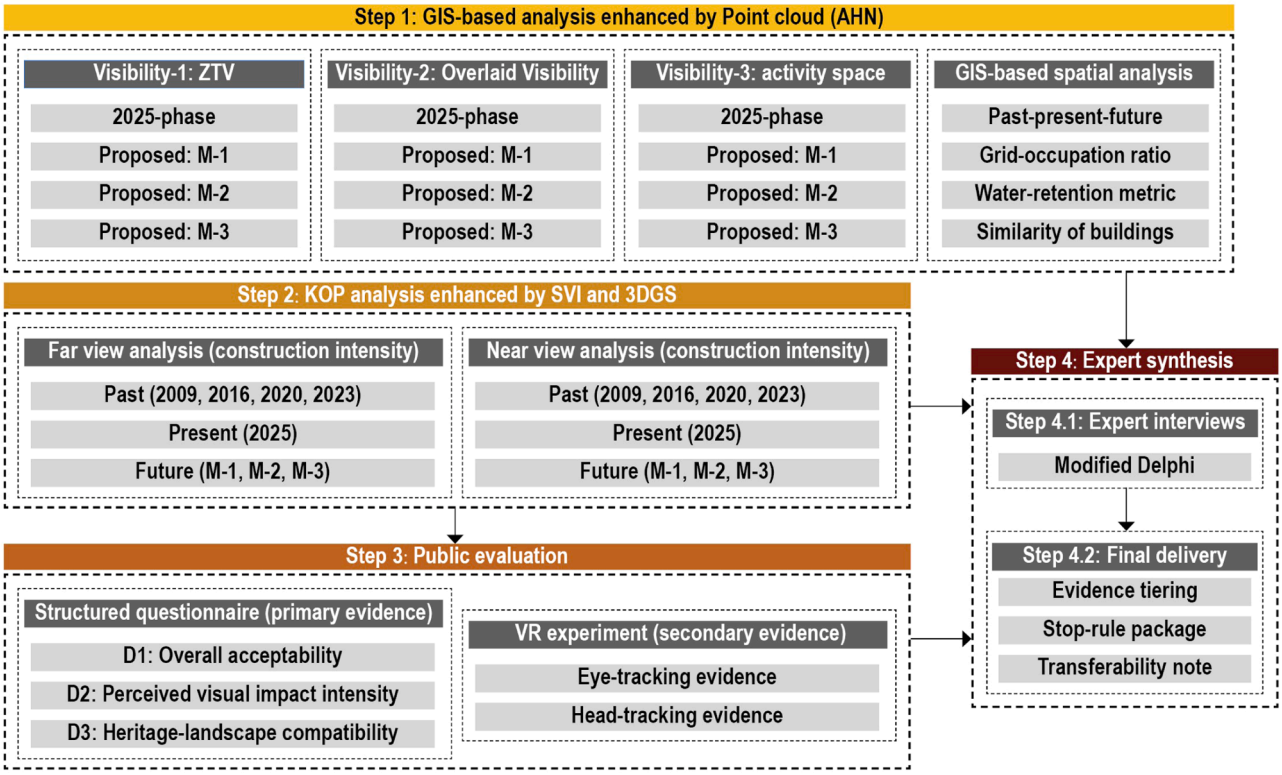

Fig. 3. The VIA workflow for the case study: GIS–AHN point cloud analysis, KOP evaluation (SVI/3DGS), Public appraisal, and expert synth.

Fig. 4. Study-area construction context and prototypes: Three development scenarios (M-1–M-3) in Middenbeemster.

were distributed across building façades and roof surfaces and used in the cumulative viewshed computation, so the resulting rasters represent where building surfaces are visible from the landscape. Building-surface sample points used surface elevations from the integrated point cloud-derived model to represent façade and roof heights. The same occluding surface definition and analysis parameters were applied to the baseline and all scenarios.

For each scenario, we report both the total number of visible raster cells and the counts of visible cells by visibility level (low, medium, high) using the same receptor sets and parameters to ensure strict comparability across conditions. Given the open Dutch setting (open landscape and scale of the research site is within 10-km), distance-decay weighting is not applied at this stage (Pbl.NL). Distance effects are addressed through interpretation and stratification, including route-based exposure along everyday movement corridors and near versus far KOP evidence in the eye-level module.

(c) Spatial analysis-1 (GIS-4): To capture how new construction infills the Beemster's rectangular dike–canal–parcel grid, scenes were classified into buildings, polder (open agricultural land), and water. Infill magnitude was quantified using a land-domain grid-occupation ratio (GOR), calculated as the building area divided by the sum of building area and polder area (i.e., water excluded from the denominator). Because water is structurally stable and not the intended infill target, it was evaluated separately using a baseline-anchored water-retention metric: a fixed baseline water mask (derived from AHN-5) was kept constant, and each period/scene reports the share of that baseline water surface that still overlaps with water in the current scene. This baseline-anchored check focuses interpretation on whether the historic canal geometry and open corridors remain legible.

4.2. Enhanced KOP analysis

We implement an enhanced KOP module to quantify viewpoint-based change using a single, stage-comparable indicator: projection-corrected building share in a 360° panorama. KOPs are grouped into far-views (monitoring skyline/edge exposure) and near-views (capturing internal visual dominance). The KOP evidence is organized into past–present–future phases and focuses on trajectories of building share. Across phases, viewpoints are matched by approximately the same planimetric coordinates. Each panorama is first processed with an ADE20K-trained multi-class semantic segmentation model; class shares are then obtained by extracting target classes (e.g., building and other landscape elements). To avoid projection bias, all shares are computed with solid-angle weights in the equirectangular domain so that contributions reflect viewing directions rather than raw pixel area.

(a) Past, cumulative and incremental impact: The past phase is represented by a multi-date SVI time series (2009/2016/2020/2023) at matched KOP locations, covering both far and near viewpoints. For each SVI panorama, semantic segmentation is applied and projection-corrected building share is computed; the resulting time series captures cumulative and incremental historical change in eye-level built dominance, summarized separately for far and near viewpoints.

(b) Present views based on SVI and 3DGS: For the present phase, far and near-views are represented using different sources due to coverage constraints. Far-view references are taken from the most recent available SVI panoramas (April 2025) and processed identically to the past series. For near-views, the present condition is represented by a 3DGS model constructed from field acquisition between May and June 2025. The 3DGS scene is deployed in Unity for standardized viewpoint control and 360° rendering; near-view KOP panoramas are rendered with fixed settings (including the 2.3 m camera height) and evaluated using the same projection-corrected building-share metric.

(c) Proposed scenarios M-1–M-3: For the proposed phase, near and far-views are handled separately. For far-view, we generate proposed KOP panoramas from the stitched point cloud model used in the visibility workflow and compute building share with the same projection-corrected metric. For near-view, proposed scenarios are implemented by adding planned massing to the present 3DGS (present) to create scenario environments (M-1–M-3). All proposed scenes preserve the spatial composition used in the GIS analysis, and proposed near-view panoramas are rendered in Unity using the same virtual-camera settings as the present 3DGS, enabling direct comparison of projection-corrected building share across conditions.

4.3. Public evaluation

Public evaluation was assessed via two complementary components: (i) a structured questionnaire as the primary evidence for public judgments and statistical inference, and (ii) an immersive VR perception experiment with eye- and head-tracking as secondary, mechanism-oriented evidence. The questionnaire included 68 respondents (30 native and 38 non-native, Table 3). The native/non-native grouping reflects respondent background as used in the questionnaire design and was retained because these groups represent different lived and evaluative positions from which visual acceptability may be judged. The VR experiment included 30 participants (5 native and 25 non-native, Table 4). The two samples were independent to reduce burden and limit repeat-exposure bias; inference focused on questionnaire ratings, while VR outcomes were treated as supportive evidence summarized with within-participant contrasts and uncertainty.

4.3.1. Structured questionnaire

The questionnaire was administered online in two rating blocks separated by a short break. Block 1 presented 21 near-view 360-degree panoramas at selected near-view KOPs, covering three SVI dates (2016/2020/2023) and four 3DGS conditions (2025 and M-1–M-3). Block 2 presented 14 far-view panoramas at matched far-view KOPs using the same seven temporal/scenario conditions; however, for the far-view set the 2025 condition was represented by SVI rather than 3DGS rendering. For each panorama, respondents rated three items on a 7-point threshold-centered scale with the midpoint anchored as "just acceptable": D1, Overall acceptability; D2, Perceived visual impact intensity; and D3, Heritage-landscape compatibility. After each KOP sequence, respondents were asked to select one or more perceived reasons for why the scene exceeded their tolerance threshold, or to provide an alternative reason in an open-response option.

Prior to modeling, we conducted a brief reliability/validity check of the three rating items (D1–D3). Statistical analysis accounted for repeated ratings within respondents and heterogeneity across visual stimuli (scene). Given the threshold-centered 7-point rating scale (midpoint anchored as "just acceptable") and the large number of repeated observations per respondent, we analyzed ratings using linear mixed-effects models (LMMs), treating the scale as approximately continuous to obtain interpretable effect-size estimates. Models were fitted separately for near- and far-view blocks using the same fixed and random-effects structure: rating $\sim$ period + gender + native + (1|respondent) + (1|scene), with period coded as seven levels (2016/2020/2023/2025/M-1/M-2/M-3). Inference was based on planned contrasts aligned with the study questions: temporal contrasts among SVI years (2016/2020/2023; reference = 2016) and scenario contrasts relative to the present-day condition (2025; reference = 2025) for M-1–M-3. For the far-view block, the 2025 condition was represented using SVI

Table 3
Participant information for the structured questionnaire.

Native-non	Gender	Age-group	Count
Native (n = 30)	Female (n = 10)	18–30	6
		31–44	2
		prefer not to say	2
	Male (n = 14)	18–30	8
		31–44	5
		prefer not to say	1
	prefer not to say (n = 6)	18–30	1
		prefer not to say	5
Non-native (n = 38)	Female (n = 14)	18–30	9
		31–44	5
	Male (20)	18–30	12
		31–44	8
	prefer not to say (4)	prefer not to say	4

Note: The native/non-native grouping records respondent background as used in the questionnaire design. In this study, the native group mainly comprised Dutch respondents with long-term familiarity with polder-type landscapes and nearby living environments, including respondents with extended residence experience and some who were born in such settings. The grouping was retained to reflect different evaluative positions from which visual acceptability was judged; it does not by itself specify formal local-stakeholder status in the Beemster Polder.

Table 4
Participant information for the VR perception experiment.

Group	Features	Count	Native
Age	18–25	11	2
	26–30	14	3
	31–35	5	0
Gender	Male	16	3
	Female	14	2
Education	Bachelor's	13	2
	Master's	14	3
	PhD	3	0

imagery rather than 3DGS rendering. Full coefficient tables and variance components (respondent/scene/residual) are provided in **Appendix A1**.

4.3.2. VR perception experiment

The VR perception experiment was implemented in Unity and delivered via an HTC VIVE Pro Eye headset with integrated eye-tracking (Tobii Pro Lab; 120 Hz; nominal accuracy ~0.5–1.1°). Stimuli included both near- and far-view KOP scenes under consistent virtual-camera placement and horizon alignment. Near-view stimuli combined three historical SVI time slices (2016/2020/2023) with a present-day condition (2025) and three modeled scenarios (M-1–M-3). Far-view stimuli comprised three phase conditions (2020/2023/2025), with the 2025 far-view represented using SVI imagery. Each scene was presented for 30 s with free head and eye movement. Scene order was randomized and counter-balanced; practice trials preceded the formal session, followed by a brief semi-structured interview.

Mechanism-oriented indicators were extracted as supportive measures: AOI fixation dwell-time composition and head-movement dispersion (yaw/pitch/roll; SD). AOIs (building, new construction, polder land, sky, and other) were defined using a Unity semantic mask pass. Standard quality control excluded trials with failed calibration or insufficient tracking. Given the secondary role of VR evidence, VR outcomes were used to corroborate questionnaire-attributed drivers by testing whether conditions judged as more impactful also showed increased attention to built mass/new construction and altered exploration behavior.

4.4. Expert synthesis and "when to stop"

To ensure that public opinions could be communicated and translated into structured decision-support guidance for planning and heritage landscape management, threshold setting was supported by a structured expert elicitation panel ($n = 7$) of professionals in heritage management and landscape planning (all at least Master's level). The purpose was not statistical inference, but to convert the public acceptability signals (ratings and stated reasons) into a structured stop-rule package for decision support. We used a modified Delphi-style procedure consisting of one independent round followed by a structured reconciliation meeting.

In the independent round, each expert completed a worksheet with three tasks. First, based on the public rating patterns and the respondent-reported reasons, experts assessed whether the acceptability boundary (midpoint "just acceptable" on the 7-point scale) was reliable and interpretable for decision use, and identified a candidate upper-bound "when to stop" condition (the highest-intensity condition still consistent with that boundary). Second, experts articulated what a practical stop rule should look like in application and provided their rationale (i.e., which indicators should trigger attention, review, or stopping, and why). Third, each expert proposed a candidate stop-rule package, specifying its recommended threshold or band, applicability scope, conditions for transferability, and indicative strength. These inputs were then discussed in a structured reconciliation meeting to document convergence and justified divergence.

After the independent round, a reconciliation meeting focused on resolving divergent interpretations and clarifying the intended role of each indicator in decision-making. Integration followed a conservative bracketing logic rather than arithmetic averaging, giving priority to the more precautionary expert judgments when defining the stopping anchor. Majority-supported precautionary positions were used to define the default stop anchor, while less precautionary minority positions were retained only to delimit the outer uncertainty envelope of the review band. The final output was a stop-rule set consisting of a recommended reference condition, a tiered evidence scheme distinguishing primary versus secondary indicators, and candidate threshold values reported as pragmatic reference values with an indicative uncertainty band. Transferability was documented alongside each rule element, distinguishing criteria expected to generalize to similar open polder heritage landscapes from those requiring site-specific calibration.

5. Results

5.1. GIS-based visibility analysis

The GIS-based visibility analysis comprises three interrelated components (detailed results see **Appendix-A2**): pedestrian-level visibility along surrounding roads, theoretical visibility of proposed constructions, and cumulative visibility integrating proposed and existing structures.

(a) GIS-1, Theoretical visibility (ZTV, Fig. 5): As a standalone envelope of potential new massing, M-3 attains the widest visible reach (≈8.05 M raster cells), slightly exceeding M-2 and M-1, while the baseline is smallest. High-intensity peaks are highest for the baseline (≈176k) and M-3 (≈162k), indicating that although M-3 maximizes spatial extent, the existing fabric still anchors pronounced focal nodes. Overall, ZTV suggests M-3 $\geq$ *M*-2 $>$ *M*-1 $>$ baseline in potential exposure.

(b) GIS-2, Contextual overlaid visibility (Fig. 6): With schemes inserted into the existing fabric, M-3 shows the widest overall visible coverage (≈2.06 M cells; comparable to M-1/baseline), whereas M-2 covers a smaller area but produces the highest high-intensity peak (≈62k cells; M-3 ≈ 50k). Mid/high-intensity totals remain modest across schemes, consistent with occlusion/aggregation: small articulated elements are visually subsumed by larger contiguous masses, compressing mid/high-intensity counts even when total exposure is broad. Accordingly, M-3 implies the most pervasive presence, while M-2 concentrates disturbance into localized peaks.

(c) GIS-3, Activity-based visibility (Fig. 7): From publicly accessible routes, larger values indicate more space remains visible (i.e., less obstruction). M-3 yields the most open network (Total ≈ 408,865; High ≈ 120k; Medium ≈ 125k), implying the least obstruction and the most frequent long-range encounters. M-1 follows with extensive but more fragmented corridors (High ≈ 83k). The baseline is most constrained overall (Total ≈104k) yet retains clear hotspots (High ≈ 30k). M-2 shows minimal road-legible openness (High < 1k), suggesting that its concentrated massing, while producing localized peaks in the combined view, reduces visibility along movement corridors.

Overall, M-3 is the most perceptually dominant (widest reach and highest road-legible openness); M-2 shows localized peaks but minimal road openness; M-1 yields broader, lower-intensity corridors; and the baseline remains relatively open with a few focal anchors (Table 5).

5.2. GIS-4: Spatial analysis

Over the past decade, the polder grid experienced gradual yet cumulative infill (Fig. 8a-c, Table 6). The land-domain GOR increased from 9.13 % (2015) to 10.93 % (2020) and 11.90 % (baseline), while water retention relative to the present reference remained essentially

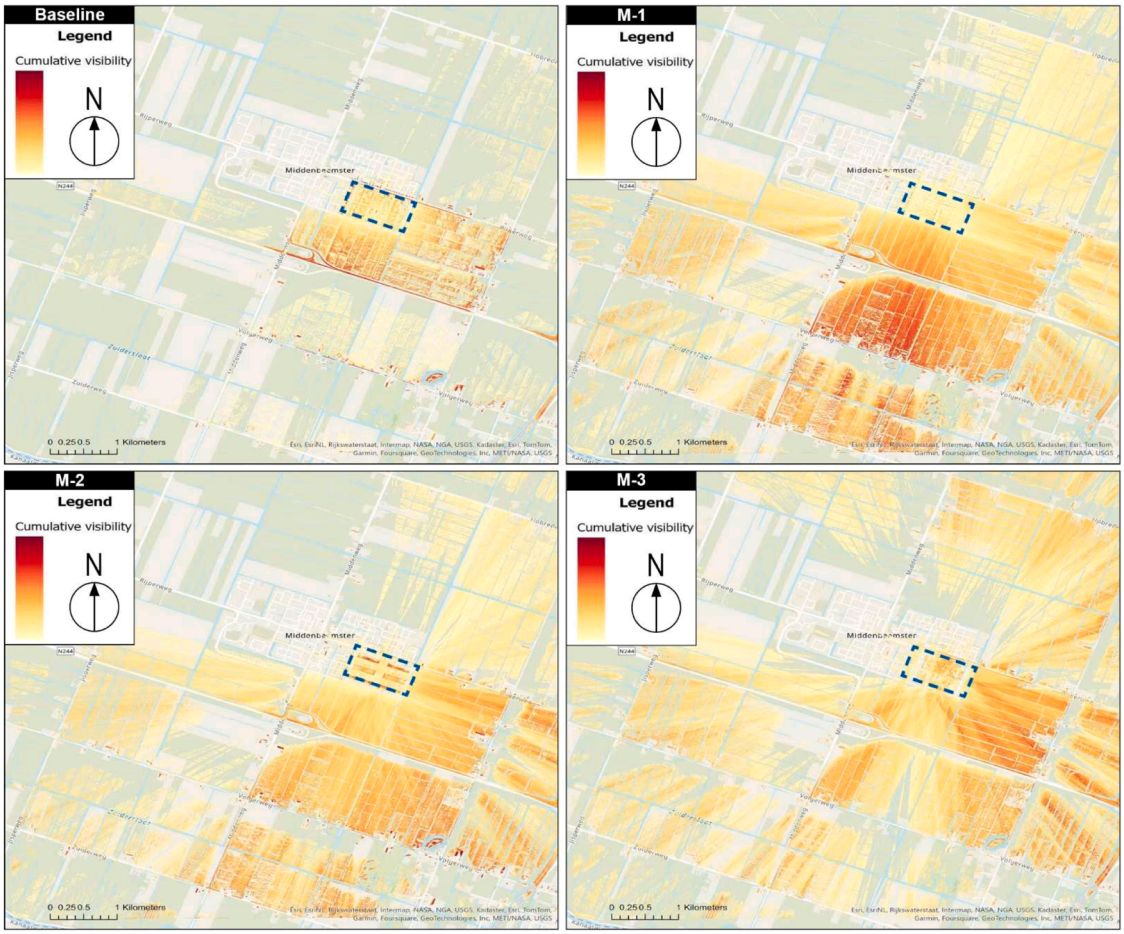

Fig. 5. Theoretical visibility maps (ZTV) for baseline model and M1/M2/M3.

complete, indicating preservation of the canal "blue skeleton." Mechanism-aware metrics likewise suggest the strip logic was largely maintained: strict Jaccard overlaps were 0.867 (2015–2020), 0.943 (2020–baseline), and 0.820 (2015–baseline), while axis-profile and edge-orientation similarity remained very high (0.983, 0.993, 0.970; row/column correlations >0.95; orientation spectra ≈1.0). Overall, the 2015–baseline trajectory reflects slow intensification without structural disruption.

Relative to the baseline, the three prospective build-out patterns diverge in magnitude and mechanism (Fig. 8d-f, Table 6). M-1 adds +0.72 pp to GOR (12.62 %) and retains 99.96 % water, with a mechanism composite of 0.987 (col 0.970; row 0.990; orientation 0.999). M-3 increases GOR by +1.80 pp (13.69) and lowers water retention to 98.53 %, with a composite of 0.954 (col 0.912; row 0.950; orientation 0.999). M-2 produces the largest land-take (+2.82 pp; 14.7 2 %) and the lowest water retention (96.48 %), with the weakest composite (0.924; col 0.842; row 0.936; orientation 0.995).

Since 2015, intensification increased land occupation while largely preserving the grid mechanism and canal integrity; however, scenario compatibility declines from M-1 → M-3 → M-2, with escalating pressure on the historic fabric.

5.3. Enhanced KOP analysis

Overall, the enhanced KOP analysis shows a consistent viewpoint-based pattern across phases and proposed scenarios. Projection-corrected building share is broadly stable in the early period, shifts around 2020 in line with the onset of site expansion, and then diverges across options with added massing intensity. In the open polder landscape, higher building share indicates a greater likelihood of perceptible construction impact, most strongly in near-field views and secondarily in far-views affecting skyline and edge exposure.

Near-view (Fig. 9): Within the SVI-covered period, near-view KOPs show limited change up to 2016 but a marked increase from 2020 onwards, indicating that the initial expansion materially altered eye-level built dominance at pedestrian scale. Under the proposed options, M-1 remains closest to current conditions, whereas M-2 and M-3 produce substantially higher building shares at multiple near-view KOPs, implying a stronger shift toward built dominance and a higher likelihood of visually prominent structures along everyday routes near the site.

Far-views (Fig. 10): To reduce seasonal bias, multi-date SVI panoramas were selected from comparable seasons wherever possible. Even with this control, far-view KOPs show little change in earlier panoramas but a pronounced decrease from 2020, plausibly reflecting increased vegetation screening along key sightlines that reduces the visible building fraction. All proposed scenarios increase far-view building share, with a modest rise under M-1 and larger increases under M-2 and M-3, consistent with greater skyline and edge exposure under more intensive massing. While far-view changes are typically less perceptually intense than near-field dominance, increases remain relevant for heritage evaluation because they signal elevated long-distance visibility and potential interruption of characteristic open sightlines.

5.4. Public evaluation results

5.4.1. Results of questionnaire

Across the seven conditions (2016, 2020, 2023, 2025 and the

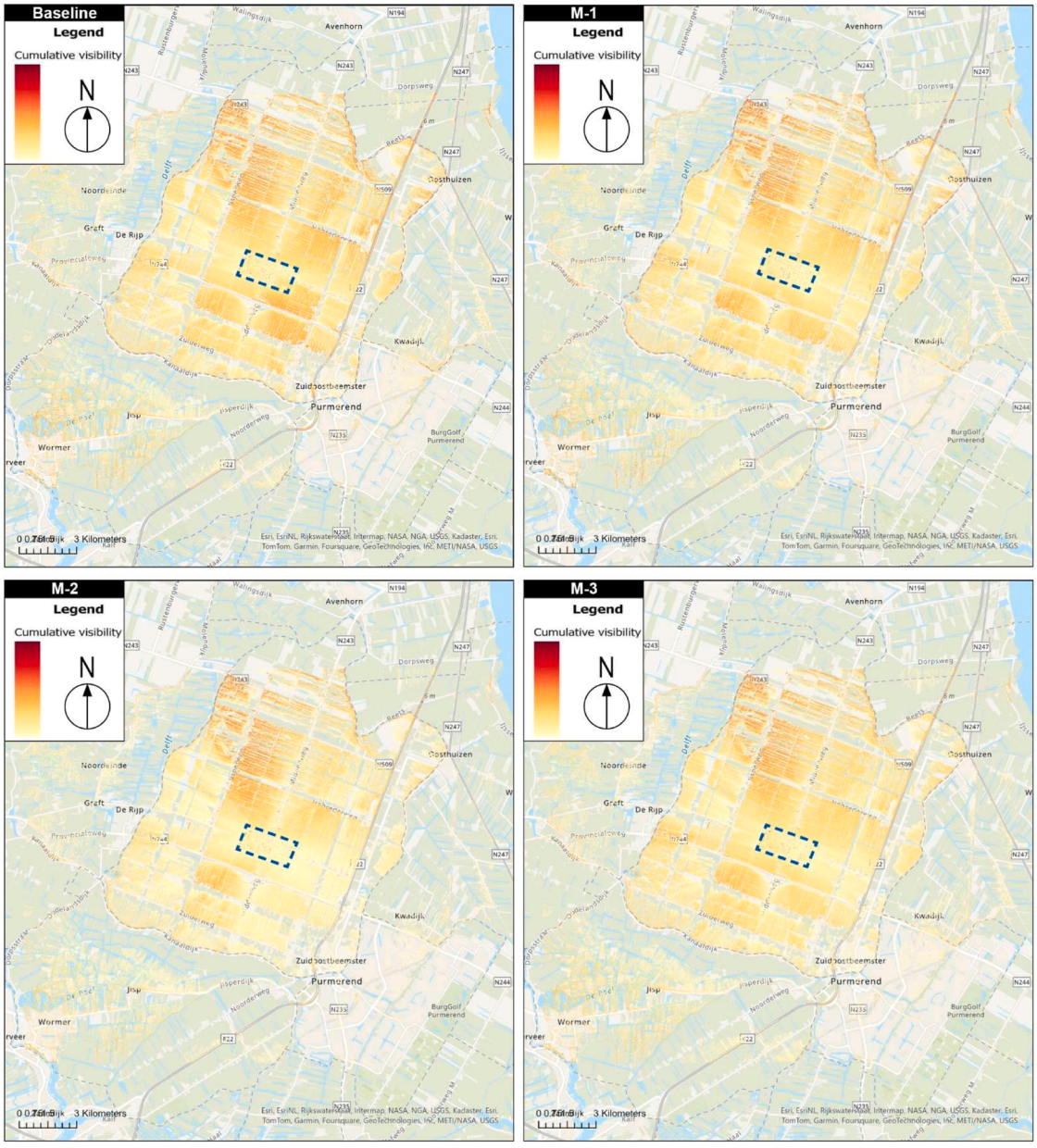

Fig. 6. Contextual overlaid visibility maps for baseline model and M1/M2/M3.

proposed scenario M-1 to M-3), all three outcomes clustered around the midpoint threshold ("just acceptable" = 4) but showed a clear near–far contrast (Table 7**,** details in **Appendix A3)**. Far-view ratings across the historical sequence (2016/2020/2023) remained close to the threshold, whereas near-view ratings varied more across periods, consistent with greater sensitivity at pedestrian scale in the open polder setting. In the present-to-future sequence, acceptability and heritage-landscape compatibility increased monotonically from 2025-phase through M-3 (with medians shifting from near-threshold toward the upper end of the scale), and impact-intensity ratings also increased, indicating stronger perceived visual impact under more intensified scenarios; the separation was strongest for M-2 and M-3 under near-view conditions.

Reliability and validity checks supported these patterns (2380 observations; Spearman rho = 0.88–0.89, $p < 0.001$; Spearman–Brown SB = 0.914–0.929). LMMs with random intercepts for respondent and scene corroborated the descriptive trends (Fig. 11): near-view scenario effects were strong and ordered (ref = 2025-phase), while far-view time-slice effects were smaller but directionally consistent (ref = 2016). Native status showed a systematic shift, with non-native respondents rating about 0.26–0.33 points lower across outcomes, indicating higher tolerance among respondents in the native group. Random effects captured stimulus-to-stimulus heterogeneity and respondent-level differences **(Appendix 1)**. Overall, viewing distance (near vs far) and period (scenario intensity or year) remained the primary drivers of public evaluations in the main models.

5.4.2. *Open-ended comment*

Open-ended responses converged on a small set of drivers of low acceptability. In the observed-change conditions (2020/2023) and the first scenario (M-1), near-view comments most often cited "construction-site" cues and excessive newness or density, frequently mentioning limited planting or green buffering and a hard, visually crowded streetscape. In far-views, respondents emphasized the overall built mass, particularly façade color and materials that read as "too new," creating a strong new–old contrast and perceived incompatibility with the wider heritage landscape. In the later scenarios (M-2/M-3), near-view

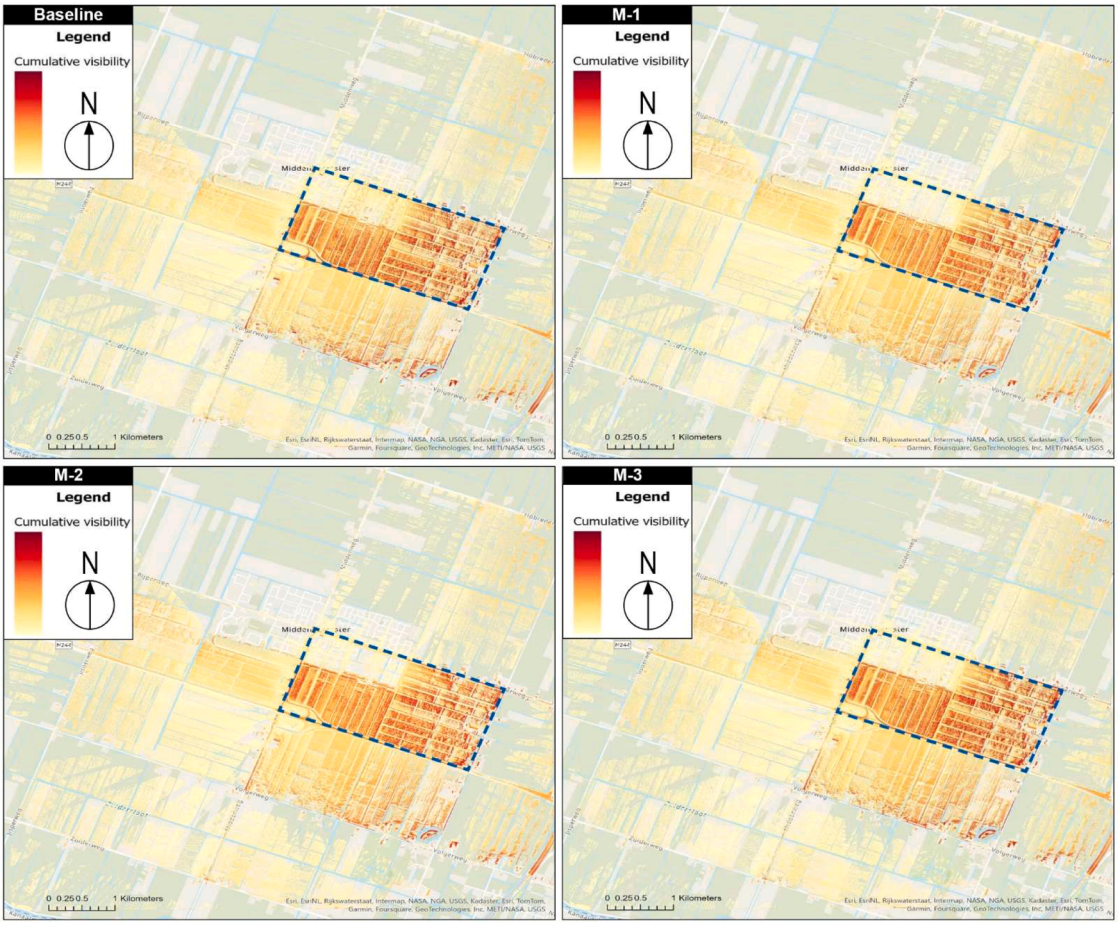

Fig. 7. Activity-based visibility maps baseline model and M1/M2/M3.

Table 5
Visibility analysis.

Filename	Low (1)	Medium (2)	High (3)	Integrated	Low %	Medium %	High %
2025_route	6734,636	846,763	176,009	7757,408	86.82	10.92	2.27
2025_context	1441,840	574,920	30,184	2046,944	70.44	28.09	1.47
2025_ZTV	61,828	12,077	29,807	103,712	59.62	11.64	28.74
M-1_route	6863,411	993,881	74,750	7932,042	86.53	12.53	0.94
M-1_context	1623,831	421,368	6742	2051,941	79.14	20.54	0.33
M-1_ZTV	179,351	101,384	83,142	363,877	49.29	27.86	22.85
M-2_route	6918,978	987,597	105,880	8012,455	86.35	12.33	1.32
M-2_context	1405,694	452,631	62,391	1920,716	73.19	23.57	3.25
M-2_ZTV	251,837	68,537	899	321,273	78.39	21.33	0.28
M-3_route	6865,362	1026,046	162,165	8053,573	85.25	12.74	2.01
M-3_context	1491,123	514,427	49,767	2055,317	72.55	25.03	2.42
M-3_ZTV	163,987	124,661	120,217	408,865	40.11	30.49	29.4

concerns shifted toward form and proximity: M-2 was more often described as blocking sightlines and interrupting openness or key corridors, whereas M-3 was criticized for height and vertical prominence that increased a sense of enclosure. Far-view comments often compared M-2 and M-3 directly, with M-2 viewed as less skyline-disruptive because its profile is more horizontally distributed.

5.4.3. Perception-based evidence

Perception-based evidence from VR eye- and head-tracking helps explain the distance-dependent patterns observed in the questionnaire and open-ended responses (details in **Appendix A3**). We summarize results by viewing distance because near and far-views rely on different visual cues and therefore point to different pathways to unacceptability. In addition, we kept comparisons source-consistent whenever possible, prioritizing 3DGS-to-3DGS contrasts for scenario effects and SVI-to-SVI contrasts for phase effects, and avoiding mixed-source baselines.

In near-views, fixation allocation shifts toward buildings and new construction across the phase sequence, while dwell time on the polder declines as open-field views become interrupted (Fig. 12, right; Fig. 13). Head-movement dispersion decreases toward the Present condition, most clearly in yaw and roll, indicating more constrained exploration when built elements dominate the near-field view. In the proposals-versus-Present comparison, attention to buildings and new construction increases from M-1 to M-3, while head-movement variability remains lower than in Present, supporting stable between-scenario contrasts.

In far-views, changes are more gradual and composition-based (Fig. 13, left). From 2020-phase to 2025-phase, building share

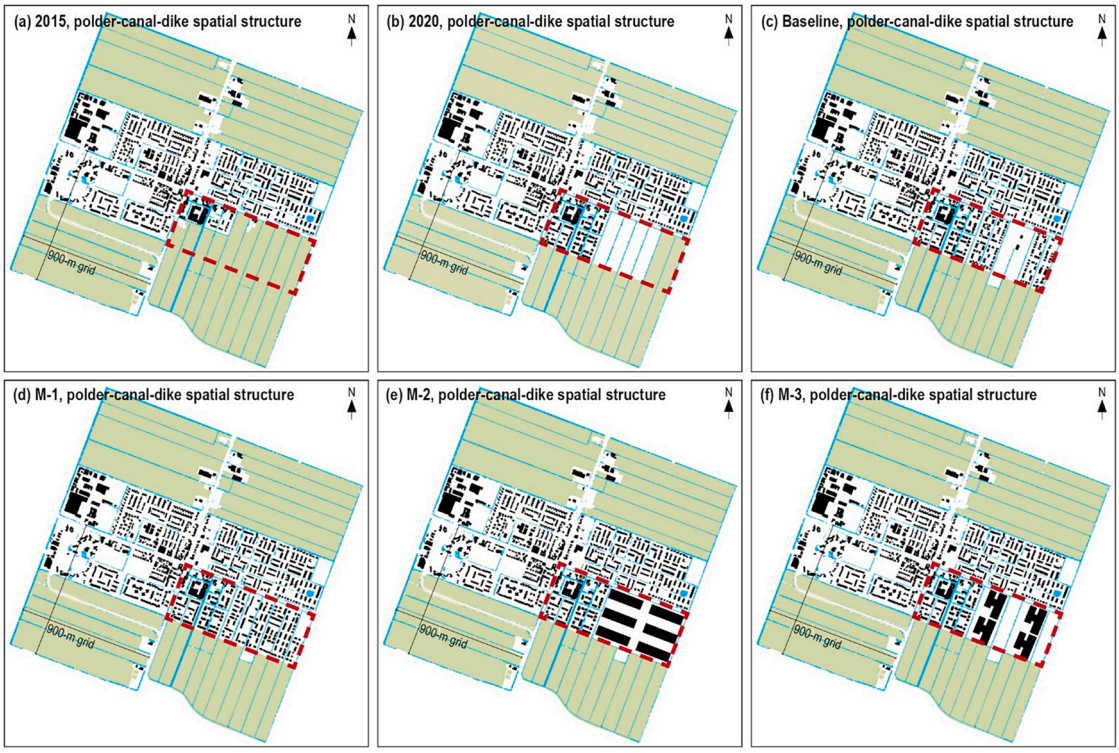

Fig. 8. GIS-based spatial analysis of the three historical period and three proposed constructions.

Table 6
Results of the evaluation with spatial indicators.

Stage	GOR (%)	Water retention vs baseline (%)	ΔGOR vs baseline (pp)	Jaccard	Jaccard (dilated)	Axis cols	Axis rows	Orient corr	Mechanism composite
2015	9.13	100.05	−2.77	-	-	-	-	-	-
2020	10.93	100.03	−0.97	-	-	-	-	-	-
Baseline	11.9	100.00	0.00	-	-	-	-	-	-
M-1	12.62	100.00	0.72	-	-	-	-	-	-
M-3	13.69	98.58	1.80	-	-	-	-	-	-
M-2	14.72	96.53	2.82	-	-	-	-	-	-
2015 vs 2020	-	-	-	0.867	0.872	0.974	0.975	1.000	0.983
2020 vs Baseline	-	-	-	0.943	0.928	0.984	0.994	0.999	0.993
2015 vs Baseline	-	-	-	0.820	0.813	0.959	0.951	1.000	0.970
Baseline vs M-1	-	-	-	0.825	0.865	0.970	0.990	0.999	0.987
Baseline vs M-3	-	-	-	0.770	0.879	0.912	0.950	0.999	0.954
Baseline vs M-2	-	-	-	0.723	0.860	0.842	0.936	0.995	0.924

increases modestly, polder salience decreases, and sky share rises; head-movement dispersion shows small upward shifts, consistent with broader scanning of skyline and edge exposure rather than inspection of construction detail. Overall, conditions that draw attention toward built mass and new construction and away from polder and vegetation align with lower acceptability and weaker heritage-landscape compatibility, with the strongest differentiation occurring in near-views.

5.5. *Integrated assessment and stop-rule formulation*

Experts were generally more conservative than the public-derived envelope. Four experts argued that expansion should stop before the 2025-phase, stressing that the prevailing delivery and building approach is already problematic in a heritage-landscape context and that alternative strategies should be pursued, such as redevelopment-first, different building forms, or stricter design governance. Two experts treated the 2025-phase as a hard stop, meaning no further expansion into M-1, and one expert accepted only a trimmed, tightly controlled M-1 under stricter design control. No expert endorsed M-2 or M-3 as acceptable endpoints. Instead, these high-heterogeneity options were widely viewed as useful stress-test extremes that reveal the impact envelope and typical failure modes, but not implementable solutions. Accordingly, the 2025-phase was taken as the conservative anchor of the stop-rule package, while the trimmed M-1 remained a narrowly conditional extension under stricter design control.

The panel also converged on a tiered hierarchy of evidence consistent with Table 8. Five experts prioritized KOP-based FOV composition, expressed as construction intensity via projection-corrected building share in panoramas and evaluated separately for near-view and far-view, as the primary reference line for review because it is directly

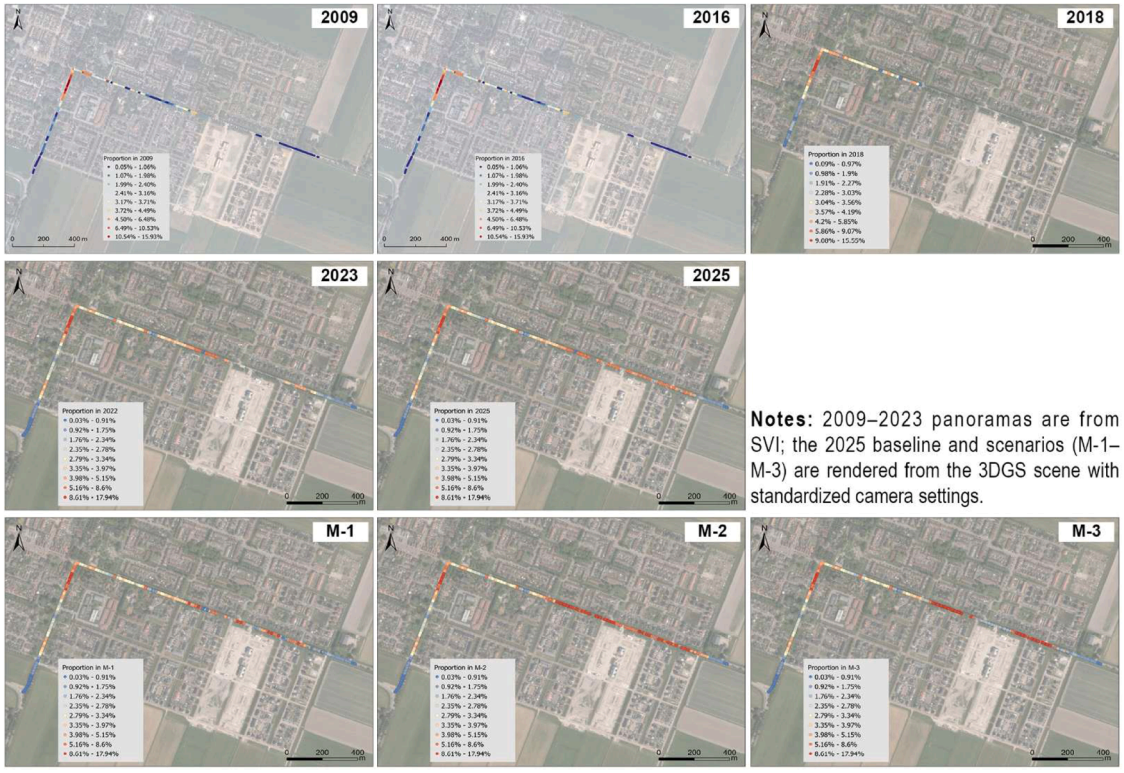

Fig. 9. The visualization of construction-intensity for near-views.

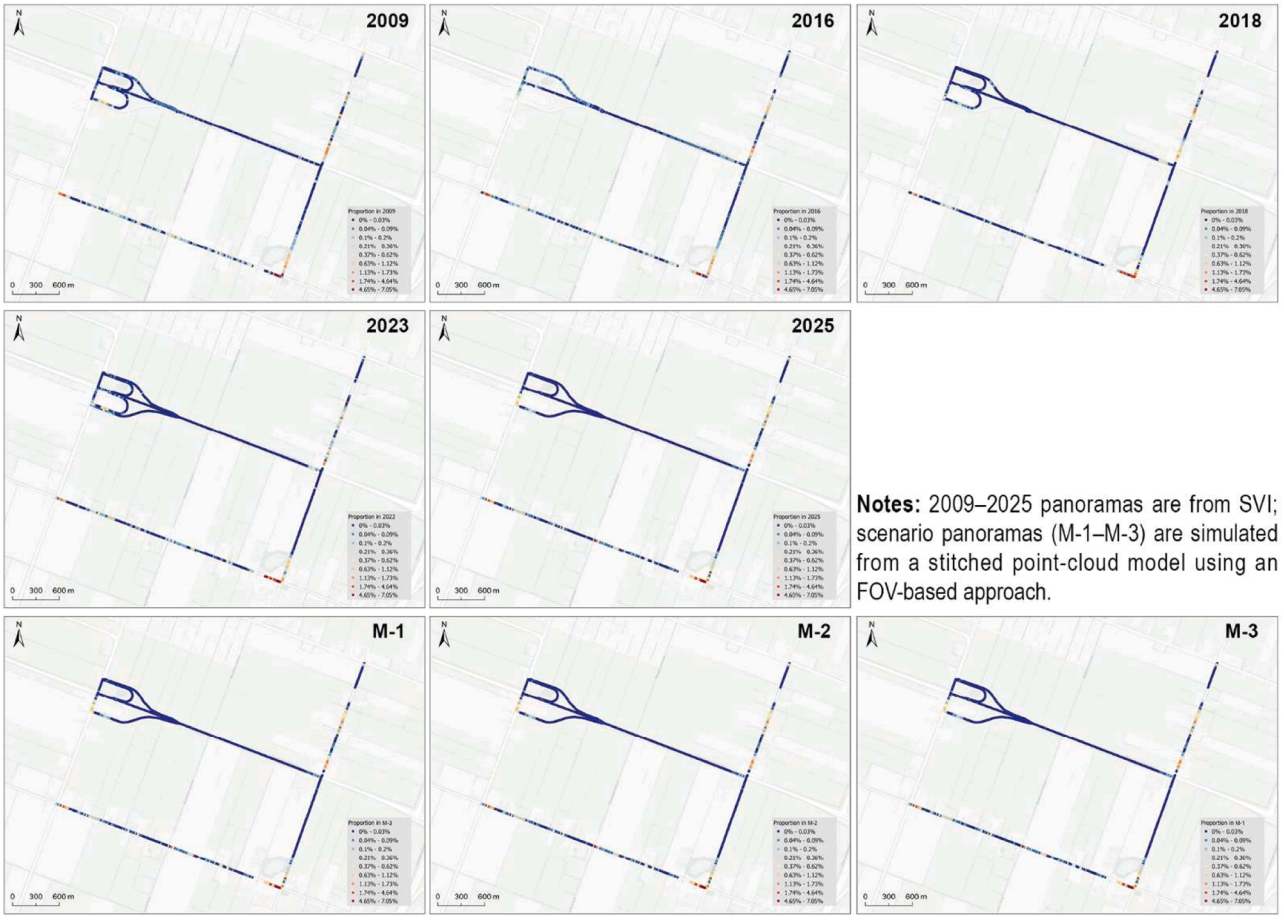

Fig. 10. The visualization of construction-intensity for far-views.

Table 7
Public-evaluation scores (mean ± SD) for near- and far-views across time (2016–2025) and scenarios (M-1–M-3).

View block	Condition	Acceptability	Impact intensity	Heritage–landscape compatibility
Near (historical)	2016	3.30 ± 0.56	2.84 ± 0.54	3.21 ± 0.55
	2020	4.90 ± 0.54	5.09 ± 0.54	5.04 ± 0.54
	2023	3.73 ± 0.64	3.71 ± 0.62	3.80 ± 0.67
Near (Present)	2025	4.62 ± 0.58	4.84 ± 0.57	4.81 ± 0.56
Near (scenarios)	M-1	5.52 ± 0.57	5.64 ± 0.55	5.56 ± 0.59
	M-2	6.57 ± 0.52	6.67 ± 0.48	6.56 ± 0.51
	M-3	6.86 ± 0.35	6.89 ± 0.31	6.85 ± 0.36
Far (historical)	2016	3.71 ± 0.52	3.88 ± 0.58	3.70 ± 0.55
	2020	3.96 ± 0.51	4.06 ± 0.53	3.98 ± 0.56
	2023	3.98 ± 0.52	4.10 ± 0.51	4.05 ± 0.53
Far (scenarios)	2025	4.18 ± 0.53	4.25 ± 0.61	4.08 ± 0.62
Far (scenarios)	M-1	4.43 ± 0.54	4.62 ± 0.52	4.32 ± 0.58
	M-2	5.57 ± 0.57	5.74 ± 0.52	5.61 ± 0.53
	M-3	6.88 ± 0.32	6.88 ± 0.33	6.74 ± 0.44

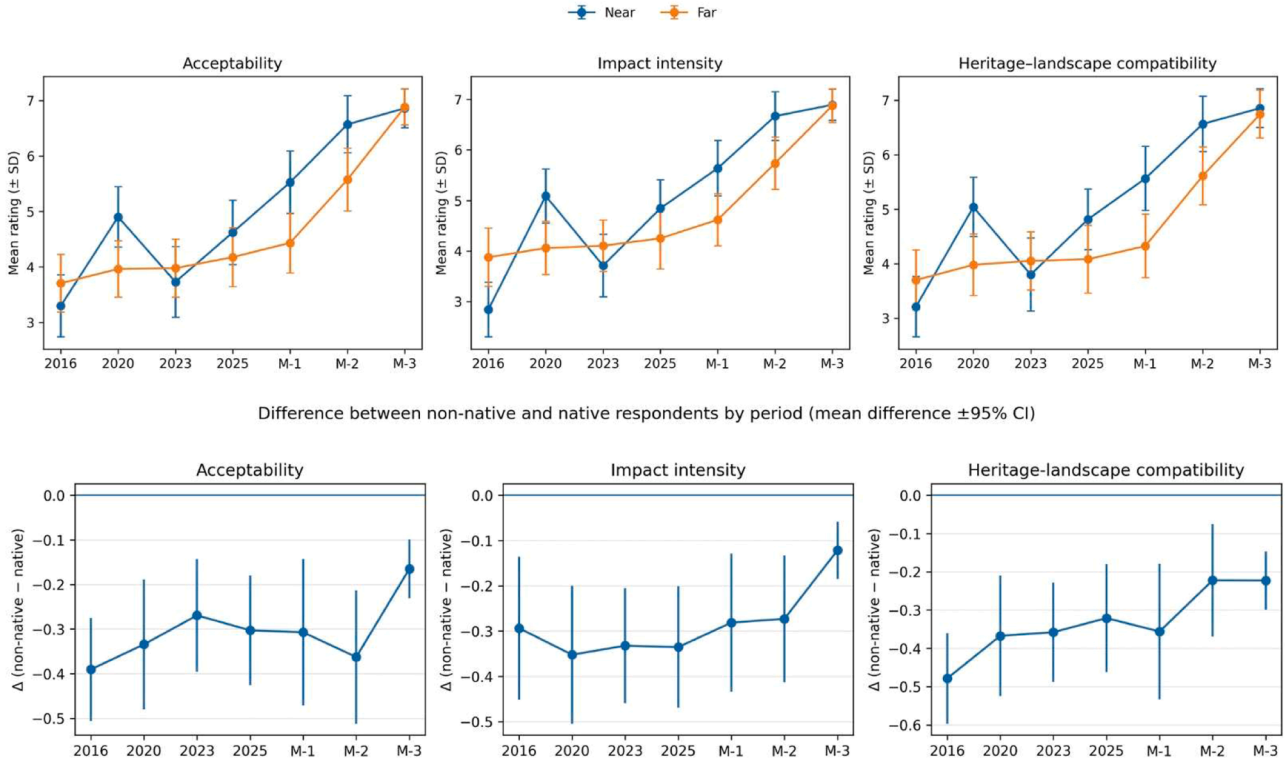

Fig. 11. Trends in public ratings (mean ± SD) for near-views vs. far-views across time and scenarios, and non-native–native differences (mean difference ±95 % CI).

interpretable and meaningful for open rural landscapes with long sightlines and skyline sensitivity. Experts stressed that this should be read as a final safeguard rather than a stand-alone rule: far-view interpretation should also consider form and contrast, while near-view interpretation requires controlling key viewing conditions such as viewing distance and road-section width; façade treatment, proportions, and materials remain complementary design considerations. All experts supported retaining VR-derived visual-behavior metrics as secondary guardrails (AOI dwell composition and head-movement dispersion), and the spatial-character indicators as a case-focused structural integrity check for safeguarding the gridded polder–canal pattern, with transferability lying mainly in the method rather than in absolute cutoffs.

Visibility was retained as an optional, scenario-specific screening layer. Experts considered it necessary to monitor but not suitable as a stand-alone stopping criterion in this low-rise incremental case; periodic checks are still needed to detect any abrupt widening of the visible envelope. For high-heterogeneity options (M-2 and M-3), ZTV was considered informative for mapping broad reach and extent, whereas for low-heterogeneity infill (the 2025-phase and M-1) experts preferred examining merged and incremental exposure and the morphology of route-based exposure after overlay with the baseline rather than applying absolute ZTV caps. Taken together, the reported bands in Table 8 are anchored at the 2025-phase, with any extension beyond that point remaining conditional and design-dependent.

6. Discussions

Conventional VIA often captures only snapshot conditions or focuses on heterogeneous projects, relying heavily on subjective judgment in low-heterogeneity contexts (Dronova, 2017). However, many rural and peri-urban heritage landscapes are not transformed by a single disruptive intervention but are gradually reshaped through cumulative, low-density encroachment (Dentoni et al., 2023; Gobster et al., 2019; Palmer, 2019). In response, this paper proposes a past–present–future VIA approach for incremental expansion in rural heritage landscapes that measures small visual changes over time and across scenarios,

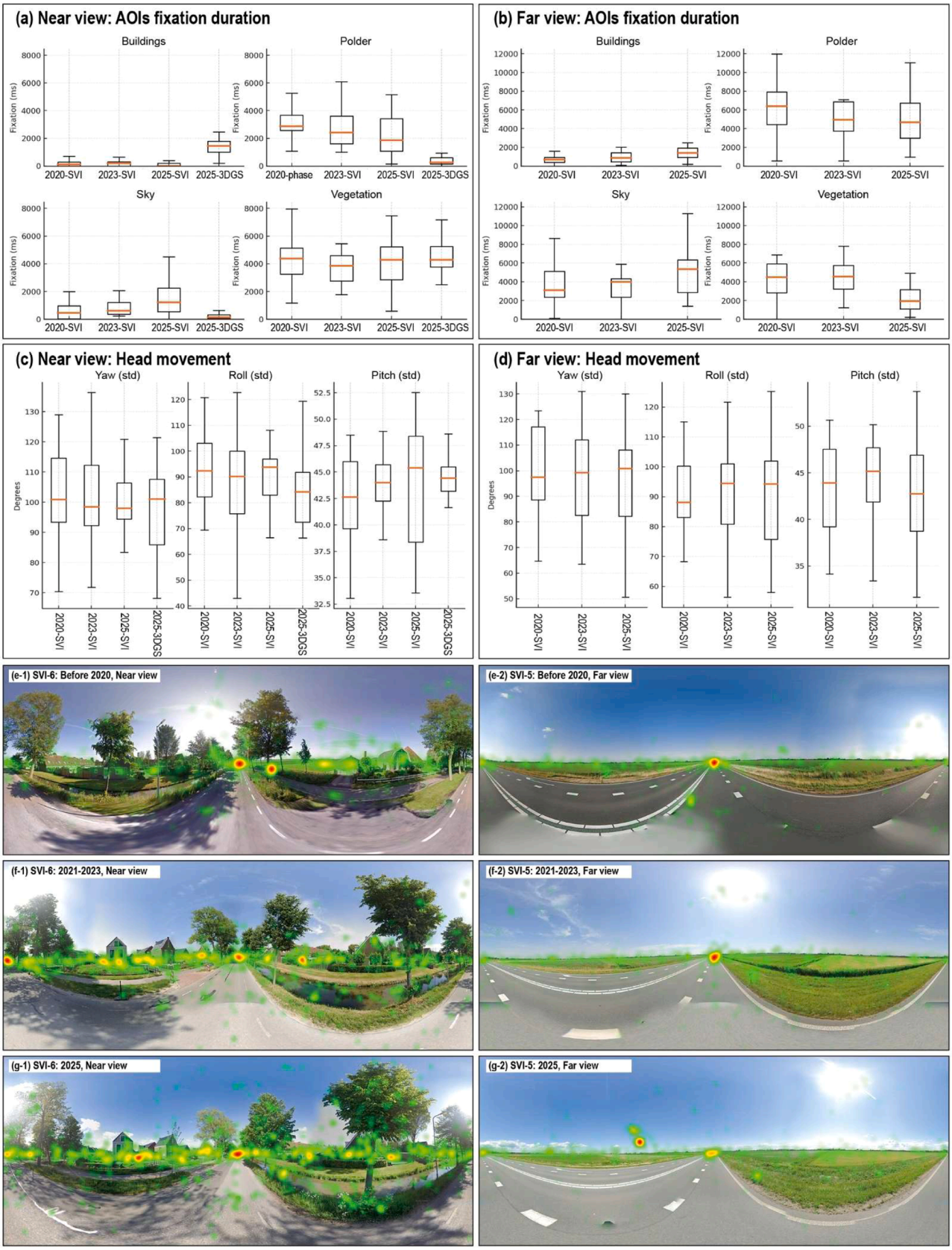

Fig. 12. Results of past to present-phase eye- and head-tracking.

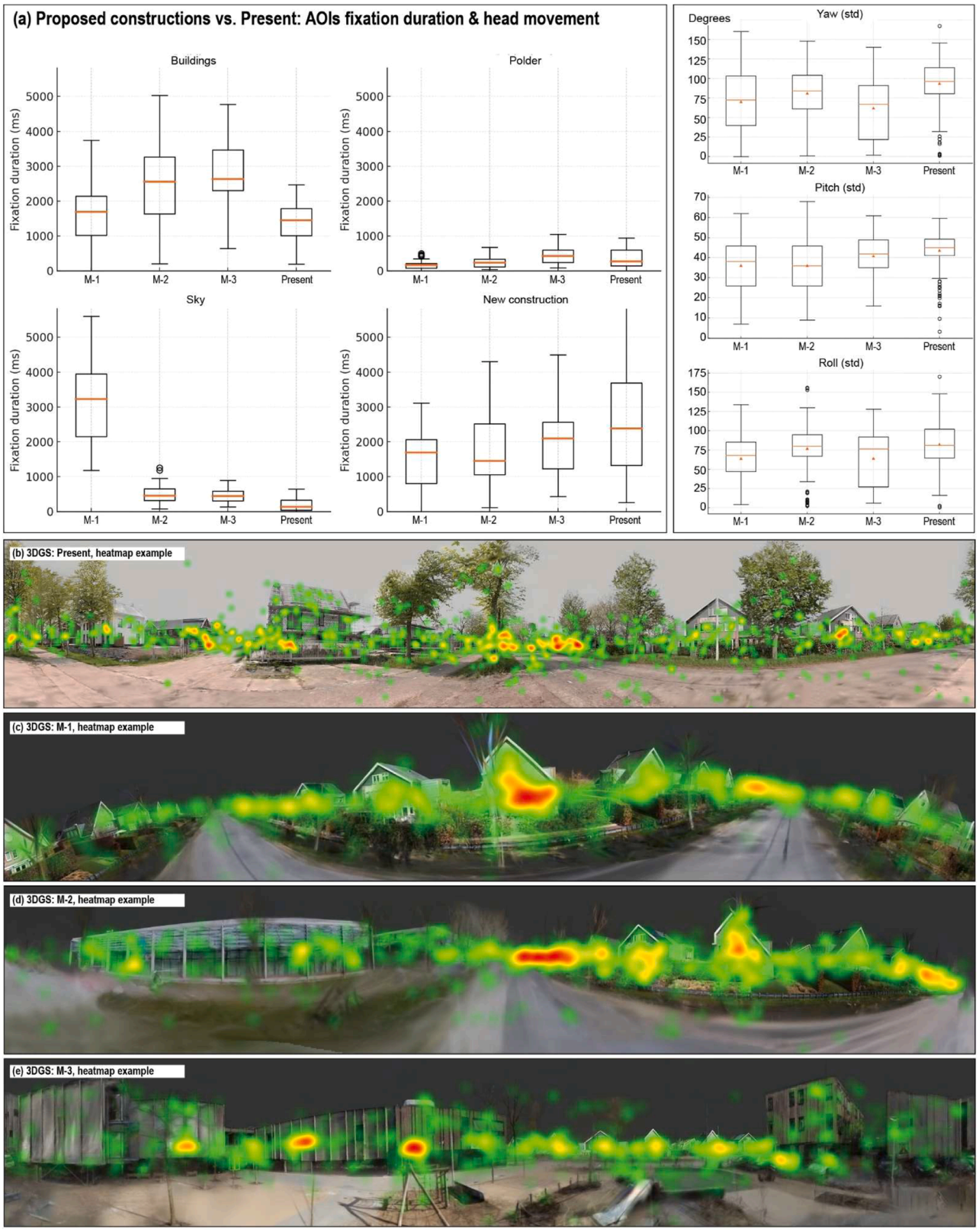

Fig. 13. Results of present-phase to proposed constructions' eye- and head-tracking.

relates them to a case-calibrated stop-rule framework for considering when further building may warrant redesign, review, or pause, and identifies practical mitigation measures. In the following discussion, we first interpret the decision implications of the case-calibrated stop-rule framework, then discuss evaluative differences under incremental impacts, summarize mitigation strategies and the role of planning controls, and finally address limitations and practical steps to strengthen transferability through local recalibration.

Table 8
Case-calibrated reference bands for the Middenbeemster stop-rule package.

Priority	Evidence line	Indicator	Threshold / rule	Role in decision
Primary	KOP – FOV composition (Near)	Construction intensity (Near KOPs; building share in FOV)	14–18 %: Attention 18–25 %: Review recommended >25 %: Mandatory audit	Applicable when the KOP viewing geometry is controlled, with the viewpoint-to-roadside built edge distance held around 8–15 m.
	KOP – FOV composition (Far)	Construction intensity (Far views; skyline/edge building share in FOV)	0.5–0.8 %: Attention 0.8–1.2 %: Review recommended >1.2 %: Mandatory audit	Applicable to KOPs with viewing distances of approximately 500–1000 m in open polder conditions. Thresholds are expressed at a smaller magnitude than near-view values.
Supporting guardrail	KOP/VR – behavior (Near-view)	Buildings' dwell (ms, p75)	p75 ≤ 1500 ms (supporting guardrail)	Supporting guardrails to corroborate near-view dominance and exploration-load; not used as a stand-alone stop-line.
		New construction dwell (ms, p75)	p75 ≤ 2000 ms (supporting guardrail)	
		Over-exploration (p75)	p75: Yaw(std) > 108° AND Roll(std) > 96°	
		Horizontal lock-in (p75)	p75: Yaw(std) < 75° AND Roll(std) < 70°	
		Vertical lock-in (p75)	Pitch(std) > 49° AND Yaw (std) < 80°	
	KOP/VR – behavior (Far-view)	Building dwell (ms, p75)	p75 ≤ 1600 ms (supporting guardrail)	Supporting guardrails to corroborate far-view attentional capture and skyline fixation; not used as a stand-alone stop-line.
		Lock-in (p75)	p75: Yaw(std) < 80° AND Roll(std) < 80°	
Case-focused	Spatial characters	ΔGOR vs baseline (pp)	≤ 0.60	Case-calibrated integrity checks (baseline-anchored). Reference triggers only, not stand-alone stop-lines; method-transferable, cutoffs local.
		Mechanism composite vs baseline	≥ 0.95	
		Water retention vs baseline	≥ 0.95	
		Jaccard vs baseline	≥ 0.80	
Required check	GIS visibility (no hard threshold here)	High-heterogeneity (M-2/M-3): ZTV reach/ extent	No stop-threshold; use as screening of "impact envelope"	Wide reach → treated as exceeding extreme exposure envelope
		Low-heterogeneity (2025+M-1): merged exposure & route-based morphology	Report incremental exposure (Δ) vs 2025; no cap	(screening judgement) Used in expert adjudication; some experts judged M-1 beyond local carrying range (diverging from public signal)

Note: These numeric bands are locally derived and calibrated to the Middenbeemster case. They are intended as context-specific reference ranges for review within this study rather than fixed operational thresholds. They were derived through a conservative bracketing of expert judgements anchored to the 2025-phase and the narrowly conditional extension toward a trimmed M-1 scenario. Application to other sites requires local re-parameterization against baseline conditions and locally plausible scenarios. They should not be interpreted as fixed or uniquely determined thresholds.

6.1. Decision implications: A case-calibrated stop-rule framework

The past-present-future VIA approach supports the derivation of a case-calibrated stop-rule framework for incremental expansion in rural heritage landscapes. By situating assessment within a temporal sequence, cumulative change becomes measurable rather than implicit, allowing decision-support reference bands to be related to observed structural shifts instead of assumed aesthetic limits. In this study, the stop-rule package is anchored in the point at which incremental development begins to produce a consistent departure from the inherited landscape framework.

This framework is informed through convergence across multiple evidence layers. Spatial similarity metrics trace parcel-level shifts in grid configuration and land-built proportion (Niesterowicz & Stepinski, 2016; Sertel et al., 2018). Visibility diagnostics enhanced through point cloud-supported modeling improve exposure accuracy beyond conventional DEM-based viewsheds and reduce bare-earth overestimation bias (Cimburova & Blumentrath, 2022; Zong et al., 2021). Although visibility values in the present case have not yet crossed a definitive limit, the geometric precision achieved through point cloud integration provides sufficient resolution to detect emerging structural imbalance before more pronounced transformation occurs. Activity-space and route-based visibility further relate exposure to encounter frequency, linking spatial change to experienced impact (Kissling et al., 2023). Immersive 3DGS-VR experiments add a complementary behavioral dimension. Eye- and head-tracking record sustained attention and dwell time, offering measurable indicators of visual salience that support and cross-validate questionnaire and interview findings (Y. Yu et al., 2025). The stop-rule package is therefore informed by convergence between spatial deviation and behavioral response rather than by a single metric.

The logic of defining such a boundary aligns with planning traditions that preserve rural structure through articulated containment frameworks. In the Netherlands, protection of the Green Heart demonstrates how recognition of a spatial envelope can prevent cumulative fragmentation while accommodating surrounding urban growth (Kühn, 2003; Romanazzi et al., 2023). Applied to the Beemster Polder, completion of the existing rectangular settlement outline, while maintaining proportional continuity with the historic grid, represents the outer edge of the locally compatible range within the landscape framework. Development introducing centralized or vertically accentuated forms within this envelope would likely disrupt skyline balance and move beyond the locally derived review range.

In contrast, many conventional VIA applications conclude with qualitative significance ratings or descriptive impact classes without

translating findings into decision-support reference bands. Even when quantitative indicators are reported, they are often applied independently rather than calibrated across spatial, visibility, and perceptual layers, and the question of whether such values are transferable is rarely addressed. By structuring the stop-rule framework through cross-modal convergence within a past-present-future sequence, the present study moves from impact description toward structured decision support, while recognizing that the reported numeric bands remain context-calibrated and case-specific.

6.2. Evaluative differences under incremental impacts in rural heritage landscapes

Incremental expansion in rural heritage landscapes often produces cumulative change that is difficult to judge from any single phase, which helps explain systematic differences between respondents occupying different background-based evaluative positions, together with experts.

Prior work generally suggests that background-based perceptions are shaped by place attachment and lived experience (Hummon, 1992; Trentelman, 2009), which can increase sensitivity to change (Mydland & Grahn, 2012), while attitudes are also moderated by perceived benefits and practical constraints such as housing demand and service provision (Fan, 2014). Our results follow this general pattern, with judgments in the native group more frequently expressed as conditional acceptance tied to whether change remains legible as incremental continuation rather than a rupture of the landscape framework.

Respondents in the non-native group, by contrast, often evaluate heritage landscapes through a more principle-based frame that places greater weight on symbolic integrity and authenticity (Dai et al., 2022; Jiang & Liu, 2024). In practice, this position can coexist with limited familiarity. In our study, some respondents in the non-native group required a short briefing on the site's heritage significance and basic landscape features before completing the questionnaire, yet they still tended to interpret additional encroachment as a categorical risk once the World Heritage framing was made explicit. These differences do not imply that one group is more correct than the other. Instead, they underline why both positions must be accounted for in heritage decision making. When heritage is also interpreted through everyday landscape experience, observation, attachment, and practical concern, these dimensions must also be taken seriously. Reconciling these frames is precisely where expert mediation becomes necessary.

Experts tended to be stricter for professional reasons that emphasize long-horizon structural risk and cumulative drift (Dupont et al., 2015). Although expert and lay visual exploration can differ in systematic ways (Y. Peng et al., 2026), the expert position in this case reflects a shared structural reading across Dutch and non-Dutch specialists, with relatively high agreement on what constitutes unacceptable deviation in an open polder setting. In this landscape type, the defining visual-spatial qualities include long sightlines, strong horizontality, and the legibility of a rectilinear grid of parcels, ditches, and roads. These qualities are easily weakened by centralized massing or vertical accentuation, which reduces visual permeability and shifts the perceived balance between open fields, settlement edges, and sky. This expert logic also provides a direct bridge to mitigation, because it implies that acceptability is strongly conditional on whether development form preserves openness and grid legibility (Nijhuis, 2020).

6.3. Visual impact mitigation strategies in design and planning

The case study reveals several observations that can inform the mitigation of visual impacts where new construction is unavoidable.

First, respect for local morphology is fundamental. Our results suggest that the relatively modest impact scores for the Middenbeemster expansion are partly explained by the decision to follow the historic parcel texture and strip-based rhythm. Even though the new buildings are not identical in form to older ones, adherence to similar materials and proportions preserved a sense of coherence (Antrop, 2005). This highlights the importance of design guidelines that prioritize continuity of scale, texture, and alignment with the underlying grid (HUL in Holland). In our expert interview evidence, blind-for-review emphasized that development in Dutch polder heritage landscapes should follow landscape structure and spatial logic as the primary armature, and he argued that looser, more distributed patterns with restrained height and clear permeability are more likely to sustain characteristic visual-spatial relations over time than centralized or vertically accentuated insertions.

Second, design control and planning review are important. In the Dutch planning context, residents and review bodies (e.g., Welstandscommissie) retain the right to review and advise on façade styles, reducing the likelihood of highly discordant insertions (De Somer, 2018). More broadly, this case indicates that planning controls can meaningfully influence perceived acceptability. Screening requirements, enforceable design guidelines, and mandated building styles or material palettes can reduce visual salience by limiting contrast, preserving edge conditions, and maintaining continuity with the underlying settlement logic. In incremental expansion settings, such controls do not remove impact, but they can keep development within a locally acceptable range by preventing abrupt departures that trigger low acceptability even at modest build-out levels.

Third, construction phasing can strongly influence impact perception. Both the quantitative results and perception experiments indicate that the construction phase is the most disruptive period, while completed buildings gradually weather into their context. Mitigation, therefore, includes shortening construction timelines and adopting phasing strategies that reduce visual impacts, building peripheral parcels first, or applying pre-weathered materials that immediately reduce color/brightness contrast with the surroundings.

Fourth, vegetation can be strategically employed. Eye-level perception tests confirmed that trees exceeding building height attenuate the visibility of new blocks and soften skyline discontinuities. Therefore, landscape design can serve as a proactive tool for restoring visual balance, for example, by planting tall hedgerows or aligning tree belts along parcel edges, which help mediate between new constructions, the polder landscape, and far-view skylines.

Overall, these strategies suggest that impact mitigation is not only a matter of limiting volumes, but also of sensitive design, controlled phasing, material treatment, and context-sensitive planning. Together, they provide a practicable pathway for reconciling expansion needs with protecting heritage landscapes.

6.4. Limitations

Several limitations of this paper should be acknowledged. First, although the structured questionnaire broadened public input, formally defined local-stakeholder representation in the Beemster Polder remains limited, and the VR perception experiment relied mainly on participants outside the formally local stakeholder group; accordingly, the social legitimacy of the perceptual evidence and expert synthesis should be treated as indicative rather than fully representative (Karatas & El-Rayes, 2015). Second, low-cost 3DGS and the VR toolchain introduce fidelity constraints that may affect the absolute magnitude of attention metrics; eye-tracking is also subject to common viewing tendencies such as initial central fixation, so interpretation emphasizes sustained attention and relative contrasts across conditions rather than first-fixation patterns alone. Third, SVI coverage is sparse and sensitive to seasonal factors including leaf-on and leaf-off variation and pruning, and limited 2025 records near the site further constrain phase-to-phase comparison at near-views (Sánchez & Labib, 2024). Fourth, despite point cloud improvements, visibility rasters still face masking, occlusion, and aggregation paradoxes under low-rise accretion and cannot capture perceptual dominance on their own (Palmer, 2022), which is why the framework combines ZTV with contextual overlays and perception

evidence. Finally, the numerical stop-rule bands are calibrated to a single World Heritage case and should not be treated as universally transferable constants; acceptability is not value neutral and may shift with stakeholder benefit positions, so applied use requires transparent documentation, sensitivity checks, and, ideally, multi-site validation.

In summary, these limitations suggest caution in interpreting perceptual generalizability and in transferring threshold values across sites. Future research should strengthen locally grounded stakeholder coverage, densify temporal imagery, refine low-cost 3DGS fidelity, and validate stop-rule frameworks in additional rural heritage landscapes. To improve transferability in practice, thresholds should be recalibrated locally using a shared procedure, for example by anchoring a reference condition (historically tolerated or baseline), stress-testing a small set of standardized scenarios, and translating the resulting locally acceptable range into banded stop-rule references rather than single cutoffs.

7. Conclusions

This paper presents an integrated VIA framework that tracks incremental urban and community expansion, assesses visual impacts on rural heritage and cultural landscapes, and supports the derivation of a case-calibrated stop-rule framework for considering when further construction may warrant redesign, review, or pause. The past-present-future logic makes cumulative change measurable and stage-comparable, and the decision layer is made explicit by combining point cloud-enhanced GIS diagnostics and eye-level KOP evidence with questionnaire-based public acceptability evidence across different respondent groups, complemented by in-depth expert interviews and synthesis and supported by VR-based perception metrics as secondary behavioral evidence. The framework moves beyond impact description by organizing converging evidence into a structured decision-support framework for mitigation, redesign, or pausing decisions as cumulative change approaches a locally derived review range.

Applied to the Middenbeemster expansion in the Beemster Polder, comparisons across past phases, present conditions, and three proposed build-out patterns confirm that incremental change accumulates and becomes perceptually consequential, with the strongest effects concentrated at parcel scale and near-view encounter spaces. The integrated assessment indicates a narrow, case-calibrated review range anchored at the present/2025 condition, while a trimmed, tightly controlled dispersed low-rise option (M-1) remains conditional and design-dependent; the more centralized options (M-2 and M-3) fall outside the locally derived range. Consistent with the revised decision logic, the reported bands are organized as a tiered evidence scheme, with KOP-based construction intensity as the primary reference line for review, perception indicators as supporting guardrails, spatial character metrics as case-specific reference checks to protect the polder framework, and visibility diagnostics retained as a necessary screening layer.

Beyond this case, the framework is transferable as a procedure for heritage-sensitive rural-urban fringes where change is incremental and cumulative, while the reported numeric bands should be treated as context-calibrated reference values rather than universally fixed thresholds. In practice, transferability can be strengthened through local recalibration by anchoring a reference condition, stress-testing a small set of locally plausible scenarios, and translating the resulting locally acceptable range into banded stop-rule references interpreted alongside local planning controls. Overall, the framework advances VIA toward a stage-comparable approach that can inform planning and heritage assessment in line with SDG 11, while formal local stakeholder engagement remains for future application.

Data and code availability

The AHN point-cloud datasets used in this study are publicly available via the Dutch national LiDAR program (AHN). Google Street View Imagery (SVI) is accessible through Google's platforms subject to their terms of service. Derived indicators, analysis scripts, and non-proprietary processed outputs supporting the findings are available from the corresponding author and will be made publicly available in an online repository upon acceptance. Some raw inputs (e.g., drone imagery and X-Grid datasets) are subject to third-party licensing restrictions and cannot be redistributed.

CRediT authorship contribution statement

Yuyang Peng: Writing – review & editing, Writing – original draft, Visualization, Software, Methodology, Investigation, Conceptualization. **Steffen Nijhuis:** Writing – review & editing, Supervision, Conceptualization. **Zhuoyue Wang:** Visualization, Software, Data curation. **Yingwen Yu:** Visualization, Software, Methodology, Conceptualization. **Edward Verbree:** Supervision. **Peter van Oosterom:** Supervision.

Declaration of competing interest

The authors declare that they have no known competing financial interests or personal relationships that could have appeared to influence the work reported in this paper.

Supplementary materials

Supplementary material associated with this article can be found, in the online version, at doi:10.1016/j.scs.2026.107364.

Data availability

Data will be made available on request.

References

Aimar, F. (2024). The "cultural landscape of Honghe Hani Rice Terraces": A UNESCO case study between persistence and change. In F. Aimar (Ed.), *The resilience of cultural landscapes: Perspectives from unesco world heritage sites* (pp. 189–223). Nature Switzerland: Springer. https://doi.org/10.1007/978-3-031-55861-0_7.

Antrop, M. (2005). Why landscapes of the past are important for the future. *Landscape and Urban Planning, 70*(1), 21–34. https://doi.org/10.1016/j.landurbplan.2003.10.002

Apostol, D., Palmer, J.F., Pasqualetti, M.J., Smardon, R., & Sullivan, R. (2016). The renewable energy landscape: Preserving scenic values in our sustainable future.

Assessment, M. E. (2005). *Ecosystems and human well-being: Wetlands and water*. World resources institute.

Bai, L., Li, Y., & Cen, M. (2021). Dynamic intervisibility analysis of 3D point clouds. *ISPRS International Journal of Geo-Information, 10*(11), 782. https://doi.org/10.3390/ijgi10110782

Bailoni, M., Edelblutte, S., & Tchékémian, A. (2012). Agricultural landscape, heritage and identity in peri-urban areas in Western Europe. *European Countryside, 4*(2), 147. https://doi.org/10.2478/v10091-012-0020-9

Berry, R., Higgs, G., Langford, M., & Fry, R. (2010). *An evaluation of online GIS-based landscape and visual impact assessment tools and their potential for enhancing public participation in the UK. 1st international workshop on pervasive web map*. Geoprocessing and Services.

Biljecki, F., & Ito, K. (2021). Street view imagery in urban analytics and GIS: A review. *Landscape and Urban Planning, 215*, Article 104217. https://doi.org/10.1016/j.landurbplan.2021.104217

Bishop, I. D., & Rohrmann, B. (2003). Subjective responses to simulated and real environments: A comparison. *Landscape and Urban Planning, 65*(4), 261–277. https://doi.org/10.1016/S0169-2046(03)00070-7

Bond, S., & Worthing, D. (2016). *Managing built heritage: The role of cultural values and significance*. John Wiley & Sons.

Bridgewater, P., & Rotherham, I. D. (2019). A critical perspective on the concept of biocultural diversity and its emerging role in nature and heritage conservation. *PEOPLE AND NATURE, 1*(3), 291–304. https://doi.org/10.1002/pan3.10040

Cilliers, D., Cloete, M., Bond, A., Retief, F., Alberts, R., & Roos, C. (2023). A critical evaluation of visibility analysis approaches for visual impact assessment (VIA) in the context of environmental impact assessment (EIA). *Environmental Impact Assessment Review, 98*, Article 106962. https://doi.org/10.1016/j.eiar.2022.106962

Cimburova, Z., & Blumentrath, S. (2022). Viewshed-based modelling of visual exposure to urban greenery – An efficient GIS tool for practical planning applications. *Landscape and Urban Planning, 222*, Article 104395. https://doi.org/10.1016/j.landurbplan.2022.104395

Dai, T., Li, J., Aktürk, G., & Jiao, J. (2022). The overlooked contribution of national heritage designation in City branding and tourism management. *Sustainability, 14*(14), 8322. https://www.mdpi.com/2071-1050/14/14/8322.

Daniel, T. C. (1976). *Measuring landscape esthetics: The scenic beauty estimation method, 167*. Department of Agriculture, Forest Service, Rocky Mountain Forest and Range.
De Somer, S. (2018). Taking aesthetics seriously in planning law: Seeking inspiration for Flanders in France, the Netherlands and the uk. *Journal for European Environmental & Planning Law, 15*(3–4), 333–358. https://doi.org/10.1163/18760104-01503006
Dentoni, V., Lai, A., Pinna, F., Cigagna, M., Massacci, G., & Grosso, B. (2023). A comprehensive methodology for the visual impact assessment of mines and quarries. *Environmental Impact Assessment Review, 102*, Article 107199. https://doi.org/10.1016/j.eiar.2023.107199
Desa, U. (2006). United nations department of economic and social affairs, population division. *Population and Development Review, 32*(3). https://link.gale.com/apps/doc/A152934670/AONE?u=anon~e5ec2251&sid=googleScholar&xid=3e47d12b.
Domingo-Santos, J. M., de Villarán, R. F., Rapp-Arrarás, Í., & de Provens, E. C. (2011). The visual exposure in forest and rural landscapes: An algorithm and a GIS tool. *Landscape and Urban Planning, 101*(1), 52–58. https://doi.org/10.1016/j.landurbplan.2010.11.018
Dower, B. (2020). Wind farms and solar PV panels in the landscape.
Dronova, I. (2017). Environmental heterogeneity as a bridge between ecosystem service and visual quality objectives in management, planning and design. *Landscape and Urban Planning, 163*, 90–106. https://doi.org/10.1016/j.landurbplan.2017.03.005
Dupont, L., Antrop, M., & Van Eetvelde, V. (2015). Does landscape related expertise influence the visual perception of landscape photographs? Implications for participatory landscape planning and management. *Landscape and Urban Planning, 141*, 68–77. https://doi.org/10.1016/j.landurbplan.2015.05.003
Echenique, M.H., Hargreaves, A.J., Mitchell, G., & Namdeo, A. (2012). Growing cities sustainably does urban form really matter? *Journal of the American Planning Association*, 78, 121–137.https://doi.org/10.1080/01944363.2012.666731.
Ervin, S. M. (2001). Digital landscape modeling and visualization: A research agenda. *Landscape and Urban Planning, 54*(1), 49–62. https://doi.org/10.1016/S0169-2046(01)00125-6
Falah, N., Falah, N., Solis-Guzman, J., & Marrero, M. (2025). An indicator-based framework of circular cities focused on sustainability dimensions and sustainable development goal 11 obtained using machine learning and text analytics. *Sustainable Cities and Society, 121*, Article 106219. https://doi.org/10.1016/j.scs.2025.106219
Fan, L. (2014). International influence and local response: Understanding community involvement in urban heritage conservation in China. *International Journal of Heritage Studies, 20*(6), 651–662. https://doi.org/10.1080/13527258.2013.834837
Fisher, P. F. (1993). Algorithm and implementation uncertainty in viewshed analysis. *International journal of geographical information systems, 7*(4), 331–347. https://doi.org/10.1080/02693799308901965
Florio, P., Peronato, G., Perera, A. T. D., Di Blasi, A., Poon, K. H., & Kämpf, J. H. (2021). Designing and assessing solar energy neighborhoods from visual impact. *SUSTAINABLE CITIES AND SOCIETY, 71*, Article 102959. https://doi.org/10.1016/j.scs.2021.102959
Gazzola, P., Belčáková, I., & Pauditšová, E. (2018). 1 Introduction. *Landscape impact assessment in planning processes* (pp. 1–27). De Gruyter Open Poland. https://doi.org/10.1515/9783110601558-003
Gobster, P., Ribe, R., & Palmer, J. (2019). Themes and trends in visual assessment research: Introduction to the Landscape and Urban Planning special collection on the visual assessment of landscapes. *Landscape and Urban Planning, 191*. https://doi.org/10.1016/j.landurbplan.2019.103635
Gravagnuolo, A., Angrisano, M., Bosone, M., Buglione, F., De Toro, P., & Fusco Girard, L. (2024). Participatory evaluation of cultural heritage adaptive reuse interventions in the circular economy perspective: A case study of historic buildings in Salerno (Italy). *Journal of Urban Management, 13*(1), 107–139. https://doi.org/10.1016/j.jum.2023.12.002
Habib, M., Habib, A., & Abboud, M. (2024). Multi-aspect critical assessment of applying digital elevation models in environmental hazard mapping. *Revue Internationale de Geomatique, 33*(Issue 0), 247–271. https://doi.org/10.32604/rig.2024.053857
Han, X., Li, Z., Cao, H., & Hou, B. (2025). Multimodal Spatio-temporal data visualization technologies for contemporary urban landscape architecture: A review and prospect in the context of smart cities. *Land, 14*(5), 1069. https://doi.org/10.3390/land14051069
Hummon, D. M. (1992). Community attachment. In I. Altman, & S. M. Low (Eds.), *Place attachment* (pp. 253–278). Springer US. https://doi.org/10.1007/978-1-4684-8753-4_12.
Jaeger, J.A.G., Soukup, T., Schwick, C., Madriñan, L.F., & Kienast, F. (2011). Landscape fragmentation in Europe.
Jiang, S., & Liu, J. (2024). Comparative study of cultural landscape perception in historic districts from the perspectives of tourists and residents. *Land, 13*(3), 353. https://www.mdpi.com/2073-445X/13/3/353.
Jin, X. (2023). A review of cityscape research based on dynamic visual perception. *Land, 12*(6), 1229. https://doi.org/10.3390/land12061229
Johnson, C.J., & Ray, J.C. (2021). The challenge and opportunity of applying ecological thresholds to environmental assessment decision making.
Karatas, A., & El-Rayes, K. (2015). Evaluating the performance of sustainable development in urban neighborhoods based on the feedback of multiple stakeholders. *Sustainable Cities and Society, 14*, 374–382. https://doi.org/10.1016/j.scs.2014.05.011
Kerbl, B., Kopanas, G., Leimkuehler, T., & Drettakis, G. (2023). 3D Gaussian splatting for real-time radiance field rendering. *ACM Trans. Graph., 42*(4), 139. https://doi.org/10.1145/3592433. Article.
Kissling, W. D., Shi, Y., Koma, Z., Meijer, C., Ku, O., Nattino, F., Seijmonsbergen, A. C., & Grootes, M. W. (2023). Country-wide data of ecosystem structure from the third Dutch airborne laser scanning survey. *Data in Brief, 46*, Article 108798. https://doi.org/10.1016/j.dib.2022.108798
Kühn, M. (2003). Greenbelt and Green Heart: Separating and integrating landscapes in European city regions. *Landscape and Urban Planning, 64*(1), 19–27. https://doi.org/10.1016/S0169-2046(02)00198-6
La Rosa, D., Geneletti, D., Spyra, M., Albert, C., & Fürst, C. (2018). Sustainable planning for peri-urban landscapes. In A. H. Perera, U. Peterson, G. M. Pastur, & L. R. Iverson (Eds.), *Ecosystem services from forest landscapes: Broadscale considerations* (pp. 89–126). Springer International Publishing. https://doi.org/10.1007/978-3-319-74515-2_5.
Lange, E. (2011). 99 volumes later: We can visualise. Now what? *Landscape and Urban Planning, 100*(4), 403–406. https://doi.org/10.1016/j.landurbplan.2011.02.016
Llausàs, A., Buxton, M. W., & Beilin, R. (2016). Spatial planning and changing landscapes: A failure of policy in peri-urban Victoria, Australia. *Journal of Environmental Planning and Management, 59*, 1304–1322. https://doi.org/10.1080/09640568.2015.1074888
Lu, S., Fang, C., & Xiao, X. (2023). Virtual scene construction of wetlands: A case study of Poyang Lake, China. *ISPRS International Journal of Geo-Information, 12*(2), 49. https://doi.org/10.3390/ijgi12020049
Marešová, J., Bašta, P., Gdulová, K., Barták, V., Kozhoridze, G., Šmída, J., Markonis, Y., Rocchini, D., Prošek, J., Pracná, P., & Moudrý, V. (2024). Choosing the optimal global digital elevation model for stream network delineation: Beyond vertical accuracy. *Earth and Space Science, 11*(12), Article e2024EA003743. https://doi.org/10.1029/2024EA003743
Middel, A., Lukasczyk, J., Maciejewski, R., Demuzere, M., & Roth, M. (2018). Sky View factor footprints for urban climate modeling. *Urban Climate, 25*, 120–134. https://doi.org/10.1016/j.uclim.2018.05.004
Moreno-Arjonilla, J., López-Ruiz, A., Jiménez-Pérez, J. R., Callejas-Aguilera, J. E., & Jurado, J. M. (2024). Eye-tracking on virtual reality: A survey. *Virtual Reality, 28*(1), 38. https://doi.org/10.1007/s10055-023-00903-y
Moreno Arjonilla, J., López Ruiz, A., Jiménez, J.-R., Aguilera, J., & Jurado, J. M. (2024). Eye-tracking on virtual reality: A survey. *Virtual Reality*, 28. https://doi.org/10.1007/s10055-023-00903-y
Mydland, L., & Grahn, W. (2012). Identifying heritage values in local communities. *International Journal of Heritage Studies, 18*(6), 564–587. https://doi.org/10.1080/13527258.2011.619554
Niesterowicz, J., & Stepinski, T. F. (2016). On using landscape metrics for landscape similarity search. *Ecological Indicators, 64*, 20–30. https://doi.org/10.1016/j.ecolind.2015.12.027
Nijhuis, S. (2020). The Noordoostpolder: A landscape planning perspective on the preservation and development of twentieth-century polder landscapes in the Netherlands. In C. Hein (Ed.), *Adaptive strategies for water heritage: Past, present and future* (pp. 212–229). Springer International Publishing. https://doi.org/10.1007/978-3-030-00268-8_11.
Oxman, R. (1997). Design by re-representation: A model of visual reasoning in design. *Design Studies, 18*(4), 329–347. https://doi.org/10.1016/S0142-694X(97)00005-7
Paar, P. (2006). Landscape visualizations: Applications and requirements of 3D visualization software for environmental planning. *Computers, Environment and Urban Systems, 30*(6), 815–839. https://doi.org/10.1016/j.compenvurbsys.2005.07.002
Palmer, J. F. (2019). The contribution of a GIS-based landscape assessment model to a scientifically rigorous approach to visual impact assessment. *Landscape and Urban Planning, 189*, 80–90. https://doi.org/10.1016/j.landurbplan.2019.03.005
Palmer, J. F. (2022). A diversity of approaches to visual impact assessment. *Land, 11*(7), 1006. https://doi.org/10.3390/land11071006
Peng, Y., Li, W., Nijhuis, S., Yu, Y., & Wu, Z. (2026a). Seeing heritage through green and blue: Assessing the visual influence of blue-green infrastructure (BGI) in historic urban areas (HUAs). *Environmental Impact Assessment Review, 118*, Article 108301. https://doi.org/10.1016/j.eiar.2025.108301
Peng, Y., & Nijhuis, S. (2021). A GIS-based algorithm for visual exposure computation: The west lake in Hangzhou (China) as example. *J. Digit. Landsc. Archit, 6*, 424–435.
Peng, Y., Nijhuis, S., Geng, M., & Yu, Y. (2025). Enhancing visual attribute comprehension of urban heritage landscapes using combined GIS-based visual analysis methods: West Lake as a case study. *Environmental Impact Assessment Review, 115*, Article 108032. https://doi.org/10.1016/j.eiar.2025.108032
Peng, Y., Nijhuis, S., Wu, Z., & Yu, Y. (2026b). From comparison to combination: Street view imagery (SVI) and 3D model-based analyses for urban visual environment assessment. *Landscape Architecture and Sustainability, 3*(1), Article 100034. https://doi.org/10.1016/j.las.2026.100034
Peng, Y., Nijhuis, S., Zhang, G., Stoter, J. E., & Agugiaro, G. (2022). Towards a practical method for voxel-based visibility analysis with point cloud data for landscape architects: Jichang garden (Wuxi, China) as an example. *Journal of Digital Landscape Architecture, 7*(7), 682–691.
Peng, Y., Zhang, G., Nijhuis, S., Agugiaro, G., & Stoter, J. E. (2024). Towards a framework for point-cloud-based visual analysis of historic gardens: Jichang Garden as a case study. *Urban Forestry & Urban Greening, 91*, Article 128159. https://doi.org/10.1016/j.ufug.2023.128159
Penko Seidl, N., & Golobič, M. (2020). Quantitative assessment of agricultural landscape heterogeneity. *Ecological Indicators, 112*, Article 106115. https://doi.org/10.1016/j.ecolind.2020.106115
Pereira Roders, A., & van Oers, R. (2012). Guidance on heritage impact assessments: Learning from its application on World Heritage site management. *Journal of Cultural Heritage Management and Sustainable Development, 2*(2), 104–114. https://doi.org/10.1108/20441261211273671

Proverbs, T. A., Lantz, T. C., & Heritage, G.i. T. C. D.o. C. (2020). Cumulative environmental impacts in the Gwich'in cultural landscape. *Sustainability, 12*(11), 4667. https://doi.org/10.3390/su12114667

Ravetz, J., Fertner, C., & Nielsen, T. S. (2013). The dynamics of Peri-urbanization. In K. Nilsson, S. Pauleit, S. Bell, C. Aalbers, & T. A. Sick Nielsen (Eds.), *Peri-urban futures: Scenarios and models for land use change in europe* (pp. 13–44). Berlin Heidelberg: Springer. https://doi.org/10.1007/978-3-642-30529-0_2.

RENES, H. (2019). Levende cultuurlandschappen als werelderfgoed. *Tijdschrift voor Historische Geografie, 4*(3), 168–184. https://doi.org/10.5117/THG2019.3.004.RENE

Romanazzi, G. R., Koto, R., De Boni, A., Ottomano Palmisano, G., Cioffi, M., & Roma, R. (2023). Cultural ecosystem services: A review of methods and tools for economic evaluation. *Environmental and Sustainability Indicators, 20*, Article 100304. https://doi.org/10.1016/j.indic.2023.100304

Sánchez, I. A. V., & Labib, S. M. (2024). Accessing eye-level greenness visibility from open-source street view images: A methodological development and implementation in multi-city and multi-country contexts. *Sustainable Cities and Society, 103*, Article 105262. https://doi.org/10.1016/j.scs.2024.105262

Sangiorgi, C., & Irali, F. (2012). An infrastructure fragmentation index for assessing landscape fragmentation due to transportation infrastructure.

Scazzosi, L. (2018). Rural landscape as heritage: Reasons for and implications of principles concerning Rural landscapes as heritage ICOMOS-IFLA 2017. *Built Heritage, 2*(3), 39–52. https://doi.org/10.1186/BF03545709

Sertel, E., Topaloğlu, R. H., Şallı, B., Yay Algan, I., & Aksu, G. A. (2018). Comparison of landscape metrics for three different level land cover/land use maps. *ISPRS International Journal of Geo-Information, 7*(10), 408. https://doi.org/10.3390/ijgi7100408

Soltani, A., Dehghani, A., & Azizi, P. (2025). Volumetric insights into urban growth analysis: Investigating vertical and horizontal patterns. *SUSTAINABLE CITIES AND SOCIETY, 130*, Article 106589. https://doi.org/10.1016/j.scs.2025.106589

Stalder, S., Volpi, M., Büttner, N., Law, S., Harttgen, K., & Suel, E. (2024). Self-supervised learning unveils urban change from street-level images. *Computers, Environment and Urban Systems, 112*, Article 102156. https://doi.org/10.1016/j.compenvurbsys.2024.102156

Stein, N., Watson, T., Lappe, M., Westendorf, M., & Durant, S. (2024). Eye and head movements in visual search in the extended field of view. *SCIENTIFIC REPORTS, 14*(1), 8907. https://doi.org/10.1038/s41598-024-59657-5

Tan, J., Gu, K., & Zheng, Y. (2024). Peri-urban planning: A landscape perspective. *Planning Theory, 23*(1), 42–63. https://doi.org/10.1177/14730952231178203

Trentelman, C. K. (2009). Place attachment and community attachment: A primer grounded in the lived experience of a community sociologist. *SOCIETY & NATURAL RESOURCES, 22*(3), 191–210. https://doi.org/10.1080/08941920802191712

Wang, Y., Yi, X., Wu, Z., Zhao, N., Chen, L., & Zhang, H. (2025). *View-Consistent 3D editing with gaussian splatting*, 2025. Cham: Computer Vision – ECCV 2024.

Wen, M., Wu, S., Wang, K., & Liang, D. (2025). Intergsedit: Interactive 3d gaussian splatting editing with 3d geometry-consistent attention prior. *arXiv preprint*. https://doi.org/10.48550/arXiv.2507.04961. arXiv. 2507.04961.

Wróżyński, R., Pyszny, K., & Wróżyńska, M. (2024). Reaching beyond GIS for comprehensive 3D visibility analysis. *Landscape and Urban Planning, 247*, Article 105074. https://doi.org/10.1016/j.landurbplan.2024.105074

Wróżyński, R., Sojka, M., & Pyszny, K. (2016). The application of GIS and 3D graphic software to visual impact assessment of wind turbines. *Renewable Energy, 96*, 625–635. https://doi.org/10.1016/j.renene.2016.05.016

Wu, Z., Nijhuis, S., Bracken, G., Peng, Y., Lian, J., & Zhang, H. (2026). Global multi-level mapping of visual heritage practice: Visual evaluation and management of cultural heritage. *Environmental Impact Assessment Review, 120*, Article 108404. https://doi.org/10.1016/j.eiar.2026.108404

Xia, Y., Yabuki, N., & Fukuda, T. (2021). Sky view factor estimation from street view images based on semantic segmentation. *URBAN CLIMATE, 40*, Article 100999. https://doi.org/10.1016/j.uclim.2021.100999

Xu, H., Lu, H., & Liu, S. (2024). Online street view-based approach for sky view factor estimation: A case study of Nanjing, China. *Applied Sciences, 14*(5), 2133. https://doi.org/10.3390/app14052133

Xue, S., Fang, Z., van Riper, C., Bai, Y., He, W., Wang, T., Zhou, Q., Cheng, C., & Huang, Z. (2025). Tracing spatial variations in ecological and economic benefits to support basic dimensions of wellbeing during urban expansion. *SUSTAINABLE CITIES AND SOCIETY*. , Article 106846. https://doi.org/10.1016/j.scs.2025.106846

Yu, Y., Verbree, E., van Oosterom, P., & Pottgiesser, U. (2025a). 3D Gaussian splatting for modern architectural heritage: Integrating UAV-based data acquisition and advanced photorealistic 3D techniques. *AGILE GIScience Ser, 6*, 51. https://doi.org/10.5194/agile-giss-6-51-2025

Yu, Y., Verbree, E., van Oosterom, P., Pottgiesser, U., Peng, Y., & Poux, F. (2025b). From comparison to integration: A workflow evaluation of 3D gaussian splatting and LiDAR point cloud for modern architectural heritage. *Automation in Construction, 180*, Article 106509. https://doi.org/10.1016/j.autcon.2025.106509

Yuan, G., Yuyao, W., & Miao, Y. (2024). Selecting building height control indicators of landmark skylines: A visual perception experiment. *Environment and Planning B: Urban Analytics and City Science, 52*(7), 1685–1700. https://doi.org/10.1177/23998083241304250

Zeng, C., Liu, P., Huang, L., Feng, S., & Li, Y. (2023). Features of architectural landscape fragmentation in traditional villages in Western Hunan, China. *SCIENTIFIC REPORTS, 13*(1), Article 18633. https://doi.org/10.1038/s41598-023-45099-y

Zhang, L., & Stewart, W. (2017). Sustainable tourism development of landscape heritage in a rural community: A case study of Azheke village at China Hani rice terraces. *Built Heritage, 1*(4), 37–51. https://doi.org/10.1186/BF03545656

Zhao, M., Zhang, J., & Cai, J. (2020a). Influences of new high-rise buildings on visual preference evaluation of original urban landmarks:a case study in Shanghai, China. *Journal of Asian Architecture and Building Engineering, 19*(3), 273–284. https://doi.org/10.1080/13467581.2020.1729769

Zhao, Y., Wu, B., Wu, J., Shu, S., Liang, H., Liu, M., Badenko, V., Fedotov, A., Yao, S., & Yu, B. (2020b). Mapping 3D visibility in an urban street environment from mobile LiDAR point clouds. *GIScience & Remote Sensing, 57*(6), 797–812. https://doi.org/10.1080/15481603.2020.1804248

Zong, X., Wang, T., Skidmore, A. K., & Heurich, M. (2021). Estimating fine-scale visibility in a temperate forest landscape using airborne laser scanning. *International Journal of Applied Earth Observation and Geoinformation, 103*, Article 102478. https://doi.org/10.1016/j.jag.2021.102478

Zube, E. H., Simcox, D. E., & Law, C. S. (1987). Perceptual landscape simulations: History and prospect. *Landscape journal, 6*(1), 62–80. https://doi.org/10.3368/lj.6.1.62